R. & M. No. 3387

MINISTRY OF AVIATION

AERONAUTICAL RESEARCH COUNCIL
REPORTS AND MEMORANDA

The Turbulent Boundary Layer with Suction or Injection

By T. J. BLACK, B.Sc., Whit.Schol., Grad.R.Ae.S., and
A. J. SARNECKI, M.A., Grad.R.Ae.S.
OF CAMBRIDGE UNIVERSITY ENGINEERING DEPARTMENT

LONDON: HER MAJESTY'S STATIONERY OFFICE
1965
PRICE £1 7s. 6d. NET

The Turbulent Boundary Layer with Suction or Injection

By T. J. BLACK, B.Sc., Whit.Schol., Grad.R.Ae.S., and
A. J. SARNECKI, M.A., Grad.R.Ae.S.

OF CAMBRIDGE UNIVERSITY ENGINEERING DEPARTMENT†

*Reports and Memoranda No. 3387**

October, 1958

Summary.

This report considers the turbulent boundary layer with distributed suction or injection applied normally through the surface. A bilogarithmic law of the wall is established analogous to the logarithmic law for impervious surfaces. Coles' wake hypothesis is extended to the transpiration layer and verified experimentally. The wall boundary condition is discussed briefly and possible effects of surface irregularity are examined. Finally the overall picture of the turbulent transpiration layer is discussed. It is considered that this report provides an acceptable framework for the evolution of a complete theory.

LIST OF CONTENTS

* Replaces A.R.C. 20 501.

† Dr. Black is now at the Illinois Institute of Technology (Research Institute) Chicago; Dr. Sarnecki is at the Royal Aircraft Establishment, Farnborough.

LIST OF CONTENTS—*continued*

1. *Introduction.*

Since Prandtl's original work in 1904, a large amount of investigation has been conducted concerning the problem of the boundary layer. Most of this work has been devoted to the case of flow over a solid surface. More recently, interest has been shown in the application of suction or injection through the surface, the former to maintain laminar flow or to prevent separation, the latter to provide surface cooling on the wings of high-speed aircraft or on turbine blades. The sucked

laminar layer in particular has been thoroughly investigated both theoretically and experimentally. The turbulent layer with transpiration, however, is much less amenable to mathematical treatment and little progress appears to have been made towards its solution. Moreover there is a lack of systematic experimental data which would permit the extension of existing semi-empirical theories to include the effect of transpiration.

Recently a thorough investigation of the turbulent boundary layer with transpiration has been undertaken by the Engineering Department of Cambridge University. Some results have been published by Kay[1] and Dutton[2], both of whom have demonstrated the existence of an 'asymptotic layer' (of constant thickness) with uniformly distributed suction. Kay has put forward a tentative analysis for the asymptotic layer, but this could not readily be extended to the general sucked layer, whilst it is open to theoretical objections (Section 2.1.1).

Elsewhere an attempt to provide a theory for the turbulent layer with transpiration has been made by Clarke *et al.*[3], but the neglect of an important relationship between certain parameters in this analysis resulted in a high degree of disagreement between the predicted and actual velocity profiles. Rubesin[4] has developed a theory for compressible layers with injection, but has not considered the velocity distribution in detail nor has he considered the special case of incompressible flow. Mickley and Davis[5] derived an incompressible form of Rubesin's analysis for comparison with their experimental velocity profiles, but did not develop the theory in detail, so that to date there is a lack of a complete theoretical framework into which the observed behaviour of turbulent transpiration layers may be fitted.

The purpose of this report is to present such a framework for incompressible layers at least in zero pressure gradient. Accordingly the report deals with the following:

(1) the existence of a law of the wall,

(2) the velocity distribution in the outer turbulent region,

(3) the conditions between the largely viscous sublayer and the fully turbulent region,

(4) the effects of different types of surface,

(5) the growth of the whole boundary layer with transpiration.

The law of the wall analogous to the logarithmic law for solid (impervious) surfaces is found to contain a squared-logarithmic term and this prediction is borne out well by the measured velocity profiles considered. In the outer region a velocity distribution corresponding to Coles'[6] wake law is observed. The situation is less satisfactory regarding the behaviour of the flow very near the wall. No reliable experimental data are available as measurements in this region are made extremely difficult by the small thickness of the sublayer. Consequently the theoretical predictions for the flow in this region can only be tested indirectly, *via* the values of certain parameters in the law of the wall (corresponding to the constant term in the logarithmic solid-surface law). This is particularly true of the wall region in the boundary layer on a non-homogeneous permeable wall, since the flow in it exhibits not only turbulence (time-variation) but also spatial fluctuations which cannot be measured directly by any method available at present, due to the small length-scale of the fluctuations. Similarly the ideas presented on the growth and development of the turbulent layer with transpiration are based more on intuitive reasoning than on the scanty experimental evidence.

The report is the result of many discussions between the authors, who have been investigating different aspects of the sucked turbulent layer and who had found the absence of a theoretical foundation a serious obstacle in their work.

2. *The Turbulent Wall Region.*

2.1. *Examination of Existing Theories.*

2.1.1. *Examination of Kay's theory.*—Kay[1] analyses only the asymptotic layer (i.e. one in which the flow quantities do not vary with x). He assumes a mixing length proportional to distance from the wall

$$L = \kappa y, \tag{2.1.1}$$

and combines this with (i) the vorticity transfer theory (of G. I. Taylor) and (ii) the momentum transfer theory (of Prandtl) obtaining in the two cases:

(i) $$\frac{d}{dy}\left(\frac{\tau}{\rho}\right) = \kappa^2 y^2 \frac{du}{dy}\frac{d^2u}{dy^2}, \tag{2.1.2}$$

(ii) $$\left(\frac{\tau}{\rho}\right) = \kappa^2 y^2 \left(\frac{du}{dy}\right)^2. \tag{2.1.3}$$

The equation of motion,

$$u\frac{\partial u}{\partial x} + v\frac{\partial u}{\partial y} = \frac{1}{\rho}\left(\frac{\partial \tau}{\partial y} - \frac{dp}{dx}\right), \tag{2.1.4}$$

reduces, for the asymptotic layer, to

$$v_0 \frac{du}{dy} = \frac{1}{\rho}\frac{d\tau}{dy}, \tag{2.1.5}$$

since $dp/dx = \partial u/\partial x = \partial v/\partial y = 0$, so that $v = v_0$, the normal velocity at the wall. (v_0 is negative since suction is being applied.) Hence by substituting either equation (2.1.2) or (2.1.3) in (2.1.5) and assuming

(i) $$\text{that } \frac{du}{dy} \to 0 \text{ as } y \to \infty,$$

or

(ii) $$\text{that } u \to U_1 \text{ as } \frac{du}{dy} \to 0,$$

Kay obtains the following results:

(i) $$\frac{u}{U_1} = 1 - \frac{1}{\kappa^2}\frac{v_0}{U_1}\ln\left(\frac{y}{\delta}\right), \tag{2.1.6}$$

(ii) $$\frac{u}{U_1} = 1 + \frac{1}{4\kappa^2}\frac{v_0}{U_1}\ln^2\left(\frac{y}{\delta}\right). \tag{2.1.7}$$

Of these formulae equation (2.1.7) is shown to disagree with experimental results, whilst (2.1.6) shows satisfactory agreement with Kay's results, which give a reasonably linear plot in the graph of $(1-u/U_1)$ against $\ln(y/\delta)$. Sarnecki's measurements in a layer which is very close to asymptotic conditions do not confirm this linear-logarithmic formula. It must be pointed out that Kay's assumption $du/dy \to 0$ as $y \to \infty$ (used to eliminate one of the constants of integration) is unsound when applied to his formula, since he considers a boundary condition well outside the range of application of his theory, for, as $y \to \infty$, equation (2.1.6) gives $u \to \infty$ and the value of its derivative at that limit is insignificant.

Also, in the derivation of equation (2.1.7) Kay assumes that the relationship $L = \kappa y$, (2.1.1), holds throughout the thickness of the boundary layer which makes an unnecessarily restrictive

hypothesis as will be shown below. It will also be shown that Kay's analysis is restricted to the special case of asymptotic conditions which, as has been demonstrated by Dutton[2], is not as readily attainable in turbulent as in laminar boundary layers with suction. The formulae (2.1.6) and (2.1.7) cannot hold for non-asymptotic conditions, in particular at low values of suction, since as $-v_0 \to 0$ they both yield $u/U_1 = \text{const.}$, whatever the behaviour of δ. {The mixing-length coefficient κ cannot vanish, as can be seen from equations (2.1.2), (2.1.3).}

2.1.2. *Examination of the theory of Clarke, Menkes and Libby.*—Clarke, Menkes and Libby[3] consider the general turbulent boundary layer with constant pressure on a permeable wall and point out that in the neighbourhood of the wall the term $v_0\,\partial u/\partial y$ is very much larger than $u\,\partial u/\partial x$ {or $(v-v_0)\,\partial u/\partial y$} and so the boundary-layer equation (2.1.4) reduces to a form identical with (2.1.5)

$$v_0 \frac{\partial u}{\partial y} = \frac{1}{\rho}\frac{\partial \tau}{\partial y}. \tag{2.1.8}$$

They use the assumption of the momentum transfer theory, (2.1.3) and obtain (with slightly different notation)

$$v_0 \frac{\partial u}{\partial y} = \kappa^2 \frac{\partial}{\partial y}\left[y^2 \left(\frac{\partial u}{\partial y}\right)^2\right]. \tag{2.1.9}$$

Integration of equation (2.1.9) yields the result

$$\frac{u}{U_\tau} = A + B \ln\left(\frac{U_\tau y}{\nu}\right) + \frac{1}{4\kappa^2}\frac{v_0}{U_\tau}\ln^2\left(\frac{U_\tau y}{\nu}\right). \tag{2.1.10}$$

Clarke *et al* use the equation (2.1.10) in that form, i.e. with *two* arbitrary constants {as demanded by (2.1.9) which is of second order}. They point out that for $v_0 \to 0$ the equation (2.1.10) reduces to the form

$$\frac{u}{U_\tau} = A + B \ln\left(\frac{U_\tau y}{\nu}\right), \tag{2.1.11}$$

the accepted logarithmic law for solid flat plates. In the absence of experimental data for the boundary layer with suction or blowing they accept the solid plate values for A, B and κ in their analysis of experimental profiles with injection and obtain poor agreement. Although Clarke *et al* recognise that A, B and κ should in general depend on v_0/U_τ, they apparently overlook the relationship between them which is implicit in the theory, as shown below.

2.1.3. *Examination of Rubesin's theory and Mickley and Davis' analysis.*—Rubesin[4] deals with compressible flow and obtains the velocity distributions in the sublayer and in the turbulent region near the wall. His basic assumptions are, once again, the predominance of the $v_0\,\partial u/\partial y$ term in equation (2.1.4) and the momentum transfer theory with linear mixing length, (2.1.1), (2.1.3). The two laws (sublayer and turbulent) are accepted as holding on either side of a transition point ($y = y_a$), at which the velocities and shear stresses {$\mu\,\partial u/\partial y$ and $\rho\kappa^2 y^2\,(\partial u/\partial y)^2$ in the two cases} are matched. These assumptions lead to the following (u, y) relationships:

$$\text{Sublayer } (0 < y < y_a): y = \int_0^u \frac{\mu\,du}{\rho_0 v_0 u + \tau_0}, \tag{2.1.12}$$

$$\text{Turbulent region } (y > y_a): y = y_a \exp \int_{u_a}^u \frac{\kappa \rho^{1/2}\,du}{\sqrt{\rho_0 v_0 u + \tau_0}}, \tag{2.1.13}$$

with y_a to be determined empirically.

The integrations are carried out by Mickley and Davis[5] for the incompressible layer, (i.e. with $\rho_0 = \rho$, $\mu = \nu\rho$, constants, and writing $\tau_0 = \rho U_\tau^2$). They obtain the following formulae:

$$\text{Sublayer}: \frac{U_\tau y}{\nu} = 2\frac{U_\tau}{v_0}\ln\left(1 + \frac{v_0 u}{U_\tau^2}\right), \tag{2.1.14}$$

$$\text{Turbulent region}: \ln\frac{U_\tau y}{\nu} - \ln\frac{U_\tau y_a}{\nu} = 2\kappa\frac{U_\tau}{v_0}\left[\left(1 + \frac{v_0 u}{U_\tau^2}\right)^{1/2} - \left(1 + \frac{v_0 u_a}{U_\tau^2}\right)^{1/2}\right]. \tag{2.1.15}$$

Mickley and Davis use this form of the equation in their comparison of theory with experiment, plotting y logarithmically against $(1 + v_0 u/U_\tau^2)^{1/2}$ and obtaining fairly good agreement with straight lines of the predicted slope $2\kappa U_\tau/v_0$ for the turbulent region with U_τ obtained from momentum considerations.

This treatment is unduly restrictive, for whereas a linear graph may in general be used to determine two unknown quantities (*via* the slope and intercept), here only the inner boundary condition (y_a or equivalently u_a) can be deduced from the experimental line, since the slope is predetermined. Admittedly any variations in slope can be interpreted as variations in the mixing coefficient κ, but there are good grounds for assuming κ to be a universal constant in two-dimensional flows, even though some disagreement may exist as to its actual value. (*See* Appendix I.)

The method developed in this paper is also based on a mixing-length analysis, but leads to a different linear plot of velocity distributions which allows both the inner boundary condition and the local skin friction to be determined from the velocity profile.

2.2. *Mixing-Length Theories with Linearly Varying Mixing Length Applied to Constant-Pressure Boundary Layers on Continuously Permeable Walls.*

2.2.1. *Equation of Motion: velocity-shear relationship.*—The boundary layer under consideration is taken to be incompressible, two-dimensional and obeying Prandtl's equation:

$$u\frac{\partial u}{\partial x} + v\frac{\partial u}{\partial y} = \frac{1}{\rho}\left(\frac{\partial \tau}{\partial y} - \frac{dp}{dx}\right), \tag{2.2.1}$$

and the continuity equation:

$$\frac{\partial u}{\partial x} + \frac{\partial v}{\partial y} = 0 \tag{2.2.2}$$

with the shear

$$\frac{\tau}{\rho} = \nu\frac{\partial u}{\partial y} - \langle u'v'\rangle. \tag{2.2.3}$$

The condition at the boundary is

$$u = o,\ v = v_0 \text{ at } y = 0. \tag{2.2.4}$$

v_0 is greater than zero in the case of injection, less than zero for suction.

Sufficiently close to the wall $\partial u/\partial y$ is large compared with u, $\partial u/\partial x$ and $(v - v_0)\left[= -\int_0^y \partial u/\partial x\, dy\right]$, so that the momentum transport $u\,\partial u/\partial x + v\,\partial u/\partial y$ is very nearly equal to $v_0\,\partial u/\partial y$, and in the absence of a pressure gradient the equation of motion (2.2.1) takes the form

$$v_0\frac{\partial u}{\partial y} = \frac{1}{\rho}\frac{\partial \tau}{\partial y}. \tag{2.2.5}$$

This equation is the exact analogue of the wall region assumption

$$0 = \frac{1}{\rho}\frac{\partial \tau}{\partial y}, \tag{2.2.5a}$$

for layers on impervious walls.

Equation (2.2.5) becomes accurate in a larger portion of the boundary layer as $|\partial u/\partial x|/|\partial u/\partial y|$ decreases, and becomes exact throughout the asymptotic layer. Moreover in all cases it is most accurate in the immediate vicinity of the wall, where $|\partial u/\partial y|$ is largest and $|u|$, $|\partial u/\partial x|$ and $|v - v_0|$ are smallest. In particular it holds well in the laminar sublayer.

Integration of equation (2.2.5) yields the velocity-shear relationship for the vicinity of the wall

$$v_0 u = \frac{\tau - \tau_0}{\rho}. \tag{2.2.6}$$

On substituting

$$\frac{\tau_0}{\rho} = U_\tau^2, \tag{2.2.7}$$

equation (2.2.6) becomes

$$U_\tau^2 + v_0 u = \frac{\tau}{\rho}. \tag{2.2.8}$$

This equation holds both in the laminar and in the turbulent portions of the wall region and provides the justification for the simultaneous matching of u and τ at $y = y_a$ in Rubesin's analysis.

The direct integration of equations (2.2.1), (2.2.2) through the boundary layer leads to the momentum integral equation for layers with transpiration:

$$\begin{aligned}\frac{d}{dx}(U_1^2\theta) + \frac{dU_1}{dx} U_1\delta^* &= \frac{\tau_0}{\rho} + v_0 U_1, \\ &= U_\tau^2 + v_0 U_1.\end{aligned} \tag{2.2.9}$$

This equation holds generally for all two-dimensional layers without slip at the boundary. For layers with constant pressure ($dU_1/dx = 0$), the equation takes the simple form

$$U_1^2 \frac{d\theta}{dx} = U_\tau^2 + v_0 U_1. \tag{2.2.9a}$$

2.2.2. *Vorticity transfer theory with $L = \kappa y$.*—The assumption of the vorticity transfer theory is that

$$\frac{1}{\rho}\frac{\partial \tau}{\partial y} = \kappa^2 y^2 \frac{\partial u}{\partial y}\frac{\partial^2 u}{\partial y^2}. \tag{2.2.10}$$

Equation (2.2.10) can be substituted in (2.2.5), yielding a second-order differential equation:

$$v_0 \frac{\partial u}{\partial y} = \kappa^2 y^2 \frac{\partial u}{\partial y}\frac{\partial^2 u}{\partial y^2},$$

i.e.

$$\frac{\partial^2 u}{\partial y^2} = \frac{v_0}{\kappa^2 y^2}. \tag{2.2.11}$$

Integrating (2.2.11) twice:

$$u = a + by - \frac{v_0}{\kappa^2} \ln y. \tag{2.2.12}$$

Defining δ as the value of y at which equation (2.2.12) gives $u = U_1$,

$$U_1 = a + b\delta - \frac{v_0}{\kappa^2} \ln \delta,$$

so that

$$u - U_1 = b(y - \delta) - \frac{v_0}{\kappa^2} \ln \frac{y}{\delta},$$

$$u = U_1 + b(y - \delta) - \frac{v_0}{\kappa^2} \ln \frac{y}{\delta}. \tag{2.2.13}$$

In equation (2.2.13) b and δ are the constants of integration. One of them may be eliminated by applying a suitable boundary condition in the region where (2.2.13) applies. Thus if the law is assumed to hold throughout the layer, i.e. even at $y = \delta$, the requisite condition may be taken as

$$\frac{\partial u}{\partial y} = 0 \text{ at } y = \delta.$$

Then

$$\left(\frac{\partial u}{\partial y}\right)_\delta = -\frac{v_0}{\kappa^2 \delta} + b = 0, \; b = \frac{v_0}{\kappa^2 \delta}, \text{ and so}$$

$$u = U_1 - \frac{v_0}{\kappa^2} \left(\ln \frac{y}{\delta} + 1 - \frac{y}{\delta} \right). \tag{2.2.14}$$

However even this condition cannot be applied with confidence in view of the common occurrence, in the outer part of the turbulent boundary layer, of a 'tail' which departs from any law holding in the inner region. Equation (2.2.14) can therefore only be applied to a layer without such a tail.

When comparing the predictions of vorticity transfer theory with experimental results, the general form (2.2.13) must be used. It should however be noted that (2.2.13) can be written in the form

$$u = \left(U_1 + \frac{v_0}{\kappa^2} \ln \frac{U_1 \delta}{\nu} - b\delta \right) - \frac{v_0}{\kappa^2} \ln \frac{U_1 y}{\nu} + by, \tag{2.2.13a}$$

and for impervious walls ($v_0 = 0$) this reduces to $u = \text{const.} + by$, i.e. a linear velocity profile, which would contradict the well established logarithmic law, so that equation (2.2.13) cannot be accepted for the whole range of v_0, though it might give good results for some special cases such as the asymptotic layer. Thus vorticity transfer theory with linearly varying mixing length is inadequate for the description of a general boundary layer with suction or injection.

2.2.3. *Momentum transfer theory with $L = \kappa y$: bilogarithmic law.*—The assumption of the momentum transfer theory is that

$$\frac{\tau}{\rho} = \kappa^2 y^2 \left(\frac{\partial u}{\partial y} \right)^2. \tag{2.2.15}$$

This can be substituted directly into (2.2.8) yielding a *first*-order differential equation:

$$U_\tau^2 + v_0 u = \kappa^2 y^2 \left(\frac{\partial u}{\partial y}\right)^2 = \left(\frac{\kappa}{v_0}\right)^2 \left(\frac{\partial [U_\tau^2 + v_0 u]}{\partial \ln y}\right)^2, \tag{2.2.16}$$

which integrates to $\sqrt{(U_\tau^2 + v_0 u)} = (v_0/2\kappa) \ln (y/d)$ with d as the one constant of integration, i.e.

$$U_\tau^2 + v_0 u = \left(\frac{v_0}{2\kappa} \ln \frac{y}{d}\right)^2. \tag{2.2.17}$$

This is the basic form of the law of the wall with transpiration under the assumptions of momentum transfer theory with linear variation of mixing length. It will be referred to as the *bilogarithmic law.*

From equation (2.2.17)

$$v_0 \frac{\partial u}{\partial y} = \frac{v_0^2}{4\kappa^2} \frac{2}{y} \ln \frac{y}{d},$$

$$\frac{\partial u}{\partial y} = \frac{v_0}{2\kappa^2 y} \ln \frac{y}{d}. \tag{2.2.18}$$

Now $\partial u/\partial y > 0$ throughout the region of validity of equation (2.2.17). Therefore for a sucked layer, $v_0 < 0$, $\ln (y/d) < 0$, $y < d$ and d is of the order of the total boundary-layer thickness. With injection, $v_0 > 0$, $\ln (y/d) > 0$, $y > d$ and d is of the order of the sublayer thickness. With suction, the velocity predicted by equation (2.2.17) has a maximum at $y = d$ whilst with injection the graph of u has a minimum at $y = d$. In neither case however can the bilogarithmic law hold at the point, since the basic assumption that the turbulent shear is much larger than the viscous shear breaks down. For

$$\tau_{\text{visc}} = \rho \nu \frac{\partial u}{\partial y} = \rho \nu \frac{v_0}{2\kappa^2 y} \ln \frac{y}{d}, \tag{2.2.19}$$

$$\tau_{\text{turb}} = \rho \kappa^2 y^2 \left(\frac{\partial u}{\partial y}\right)^2 = \rho \frac{v_0^2}{4\kappa^2} \left(\ln \frac{y}{d}\right)^2, \tag{2.2.20}$$

$$\frac{\tau_{\text{turb}}}{\tau_{\text{visc}}} = \frac{1}{2} \frac{v_0 y}{\nu} \ln \frac{y}{d} \to 0, \text{ as } y \to d. \tag{2.2.21}$$

2.3. *Application of the Bilogarithmic Law.*

2.3.1. *Methods of plotting.*—The bilogarithmic law obtained in Section 2.2.3

$$U_\tau^2 + v_0 u = \left(\frac{v_0}{2\kappa} \ln \frac{y}{d}\right)^2 \tag{2.3.1}$$

can be expected to hold in the inner turbulent region of all boundary layers with continuously distributed suction or injection, provided that

(i) the flow is nearly two-dimensional

(ii) the pressure gradient normal to the surface is negligible, i.e. Prandtl's equation holds

(iii) the laminar sublayer does not occupy a very large proportion of the boundary-layer thickness, i.e. the region in which equation (2.2.8) holds is not completely laminar.

In particular a suitable limiting form of (2.3.1) holds in the case of impervious boundaries, $v_0 = 0$. Equation (2.3.1) can be rewritten in any of the following forms

(i)
$$\frac{u}{v_0} = -\frac{U_\tau^2}{v_0^2} + \frac{1}{4\kappa^2}\left(\ln\frac{y}{d}\right)^2, \tag{2.3.2}$$

(ii)
$$\frac{u}{U_\tau} = -\frac{U_\tau}{v_0} + \frac{1}{4\kappa^2}\frac{v_0}{U_\tau}\left(\ln\frac{U_\tau y}{\nu} - \ln\frac{U_\tau d}{\nu}\right)^2,$$

i.e.

$$\frac{u}{U_\tau} = a + b\ln\frac{U_\tau y}{\nu} + \frac{1}{4\kappa^2}\frac{v_0}{U_\tau}\left(\ln\frac{U_\tau y}{\nu}\right)^2, \tag{2.3.3}$$

with

$$a = \frac{U_\tau}{v_0}(\lambda^2 - 1), \quad b = \frac{\lambda}{\kappa}, \tag{2.3.4}$$

where

$$\lambda = -\frac{1}{2\kappa}\frac{v_0}{U_\tau}\ln\frac{U_\tau d}{\nu}, \tag{2.3.5}$$

(iii)
$$\frac{u}{U_1} = -\frac{U_\tau^2}{v_0 U_1} + \frac{1}{4\kappa^2}\frac{v_0}{U_1}\left(\ln\frac{U_1 y}{\nu} - \ln\frac{U_1 d}{\nu}\right)^2,$$

i.e.

$$\frac{u}{U_1} - \frac{1}{4\kappa^2}\frac{v_0}{U_1}\left(\ln\frac{U_1 y}{\nu}\right)^2 = \left[\frac{1}{4\kappa^2}\frac{v_0}{U_1}\left(\ln\frac{U_1 d}{\nu}\right)^2 - \frac{U_\tau^2}{v_0 U_1}\right] - \left(\frac{1}{2\kappa^2}\frac{v_0}{U_1}\ln\frac{U_1 d}{\nu}\right)\ln\frac{U_1 y}{\nu}. \tag{2.3.6}$$

Equation (2.3.2) provides a universal method of plotting experimental results for comparison with theory, for when a layer satisfying the bilogarithmic law is plotted on the basis of u/v_0 against $\log y$, the resultant graph must be a parabola of fixed shape (for a given value of κ), with its axis along increasing u/v_0 and its apex at $y = d$, $u/v_0 = -U_\tau^2/v_0^2$. Thus a single standard curve would in theory be sufficient to determine both U_τ and the value of d for an experimental velocity profile, by sliding the theoretical curve over the experimental graph until a good fit is obtained. In practice this method fails because of the large range of values of u/v_0 encountered and the small curvature of the standard parabola, leading to a high degree of uncertainty over the exact location of the all-important apex.

Equations (2.3.3) to (2.3.5) present the form of the bilogarithmic law analogous to the orthodox logarithmic law for boundary layers on impervious boundaries

$$\frac{u}{U_\tau} = A + B\ln\frac{U_\tau y}{\nu} \tag{2.3.3a}$$

with

$$B = \frac{1}{\kappa}. \tag{2.3.4a}$$

The most convenient method of plotting experimental results is in the form suggested by equation (2.3.6) since the left-hand side of the equation contains only quantities which are measurable directly (the value of κ is assumed known), and the right-hand side is *linear* in $\log(U_1 y/\nu)$. In practice the best way of using equation (2.3.6) is to use not $\log y$ but a suitable multiple of it as the abscissa, as follows:

In the case of suction ($v_0 < 0$), use the substitution

$$\frac{1}{2\kappa}\sqrt{\left(\frac{-v_0}{U_1}\right)}\ln\frac{U_1 y}{\nu} = Y_s, \tag{2.3.8}$$

then equation (2.3.6) reduces to

$$\frac{u}{U_1} + Y_s^2 = (p_s^2 - n_s^2) + 2n_s Y_s, \tag{2.3.9}$$

with

$$n_s = \frac{1}{2\kappa}\sqrt{\left(\frac{-v_0}{U_1}\right)}\ln\frac{U_1 d}{\nu}, \tag{2.3.10}$$

and

$$p_s^2 = \frac{U_\tau^2}{-v_0 U_1}. \tag{2.3.11}$$

With injection ($v_0 > 0$) the substitution

$$\frac{1}{2\kappa}\sqrt{\left(\frac{v_0}{U_1}\right)}\ln\frac{U_1 y}{\nu} = Y_i, \tag{2.3.12}$$

leads to

$$\frac{u}{U_1} - Y_i^2 = (n_i^2 - p_i^2) + 2n_i Y_i, \tag{2.3.13}$$

with

$$n_i = -\frac{1}{2\kappa}\sqrt{\left(\frac{v_0}{U_1}\right)}\ln\frac{U_1 d}{\nu}, \tag{2.3.14}$$

and

$$p_i^2 = \frac{U_\tau^2}{v_0 U_1}. \tag{2.3.15}$$

The advantage of using Y rather than $\log(U_1 y/\nu)$ lies in the fact that in the graph of $u/U_1 \pm Y^2$ against Y the curves of zero velocity and full free-stream velocity ($u = 0$, $u = U_1$) are then fixed parabolae ($u/U_1 + Y_s^2 = Y_s^2, 1 + Y_s^2$ for all sucked layers; $u/U_1 - Y_i^2 = -Y_i^2, 1 - Y_i^2$ for all blown layers) independent of the actual value of v_0/U_1, so that direct comparison may be made between layers with different rates of suction or of injection, and the state of the boundary layer can be deduced from the geometry of the system of the two parabolae and the experimental straight line. Thus in the case of suction the straight line will cut, touch or not cut the parabola $u/U_1 = 1$ according as p_s^2 is greater than, equal to, or less than unity; similarly in the case of injection the straight line will cut, touch or not cut the parabola $u/U_1 = 0$ according as p_i^2 is greater than, equal to, or less than zero.

The momentum integral equation with transpiration in zero pressure gradient takes the form (2.2.9a):

$$U_1^2\frac{d\theta}{dx} = U_\tau^2 + v_0 U_1,$$

or

$$\frac{d\theta}{dx} = \frac{v_0}{U_1}\left(1 + \frac{U_\tau^2}{v_0 U_1}\right). \tag{2.3.16}$$

Thus with suction [from equation (2.3.11)]

$$\frac{d\theta}{dx} = \frac{-v_0}{U_1}(p_s^2 - 1), \tag{2.3.17}$$

and the boundary layer is growing if $p_s^2 > 1$ (experimental straight line cuts the parabola $u/U_1 = 1$). Such a layer can be termed *undersucked.*

If $p_s^2 = 1$ (line touches parabola), the boundary layer has constant (momentum) thickness and so has reached the *asymptotic* condition.

If $p_s^2 < 1$ (line does not meet parabola), the momentum thickness is actually decreasing and the layer will be called *oversucked.*

With injection (2.3.15)

$$\frac{d\theta}{dx} = \frac{v_0}{U_1}(p_i^2 + 1). \tag{2.3.18}$$

Thus with injection the boundary layer always grows and, as a rule, $d\theta/dx \geqslant v_0/U_1$, if the assumptions of the basic theory hold (two-dimensional flow, no slip). The experimental straight line then cuts the parabola $u/U_1 = 0$. It is tangential to it when the effective wall shear vanishes (i.e. $p_i^2 = 0$). This condition need not imply separation and it is shown in Section 5 that both zero and negative effective wall shear may be encountered in an unseparated layer. In the latter case the straight line fails to meet the parabola.

Typical profiles plotted as $(u/U_1 + Y_s,\ u/U_1 - Y_i)$ against Y_s, Y_i are shown in Fig. 1a (suction) and Fig. 1b (injection). Fig. 1c shows profiles, with v_0 less than, equal to and greater than zero, plotted on the more familiar basis of u/U_τ against log $U_\tau y/\nu$ to show the curvature of the 'bilogarithmic' profiles.

The relationship between the parameter λ defined by equation (2.3.5) and the constants determined from the linear plot is as follows. For suction

$$\lambda = \frac{1}{p_s}\left[n_s + \frac{1}{2\kappa}\sqrt{\left(\frac{-v_0}{U_1}\right)} \ln\left(p_s\sqrt{\frac{-v_0}{U_1}}\right)\right]. \tag{2.3.19}$$

For injection

$$\lambda = \frac{1}{p_i}\left[n_i - \frac{1}{2\kappa}\sqrt{\left(\frac{v_0}{U_1}\right)} \ln\left(p_i\sqrt{\frac{v_0}{U_1}}\right)\right]. \tag{2.3.20}$$

If U_τ^2 (and p_i^2) vanish, then the boundary layer cannot be plotted as u/U_τ against log $U_\tau y/\nu$. If U_τ^2 (and p_i^2) are negative, then U_τ is imaginary but finite and the velocity profile can be plotted in the form u/iU_τ against log $(iU_\tau y/\nu)$, $(i = \sqrt{-1})$. Equation (2.3.3) can then be rewritten

$$\frac{u}{U_\tau} = a' + b' \ln\frac{iU_\tau y}{\nu} + \frac{1}{4\kappa^2}\frac{v_0}{iU_\tau}\left(\ln\frac{iU_\tau y}{\nu}\right)^2 \tag{2.3.21}$$

with

$$a' = \frac{iU_\tau}{v_0}(\lambda'^2 + 1), \quad b' = \frac{\lambda'}{\kappa}, \tag{2.3.22}$$

where

$$\lambda' = -\frac{1}{2\kappa}\frac{v_0}{iU_\tau}\ln\frac{iU_\tau d}{\nu}. \tag{2.3.23}$$

The physical significance of the imaginary U_τ (negative wall shear) will be discussed in Section 5.

2.3.2. *The coefficients κ and λ.*—The bilogarithmic law for the turbulent boundary layer, when expressed in the form analogous to the universal law for solid boundaries, equations (2.3.3 to 2.3.5), contains two dimensionless coefficients, κ and λ. The only condition imposed on these by the basic theory is that they should be independent of wall distance y. They can vary with v_0, U_τ and type of surface employed, but in such a way that, for a smooth surface, when $v_0 = 0$ the coefficients $a\{= (U_\tau/v_0)(\lambda^2 - 1)\}$ and $b(= \lambda/\kappa)$ reduce to their universal solid-case values A and B (*see* Appendix I).

It can be argued intuitively that the mixing-length coefficient should be independent of the transpiration velocity v_0, provided v_0 is small by comparison with the longitudinal velocity in the region where the assumptions of the mixing-length theory hold. For if a slice of a mean-flow stream-tube is taken as a control volume, the mixing length in it can be described as $\kappa y'$ where κ may depend on the local curvature of the flow, and the effective wall distance y' may not be identical with y. If however v is small in the control volume, then the inclination of the stream to the wall is negligibly small, and the curvature even more so. In practice v is rarely greater than $0{\cdot}01U_1$ and u does not fall below $0{\cdot}25U_1$ in the turbulent region so that $v/u < 0{\cdot}04$ and the inclination $\alpha < 0{\cdot}04$ radians: thus y' (which might be expected to depart from y to the same extent as $\cos\alpha$ departs from 1) does not differ from y by more than $0{\cdot}1\%$. The curvature might be important if the ratio of wall distance to the radius of curvature became appreciable. However this ratio $\approx y(v/u)\,\partial\alpha/\partial y$, which is of even smaller order of magnitude than α, so that for the small values of v_0 applied in practice these considerations suggest that the turbulence in the flow is unaffected by the crossflow v. Hence there appears no reason why κ should change with v_0 from its universal solid-wall value, and if the model of a turbulent boundary layer described by mixing-length theory with $L = \kappa y$ is acceptable for solid boundaries, the condition of transpiration can be included without making the model any less accurate and with the value of κ unchanged. The solid-plate value of $\kappa = 1/B$ (*see* Appendix I) will therefore be used in all calculations.

The profile parameter λ, defined by equation (2.3.5) is essentially a constant of integration and so must be related to a boundary condition. It is in fact determined by the way in which the viscous law of the sublayer blends with the bilogarithmic law of the fully turbulent region. The laws governing the flow in this blending region are as yet uncertain. The mere superposition of viscous effects and the turbulent stresses derived from the momentum transfer theory with $L = \kappa y$, fails to predict the behaviour of the flow when $v_0 = 0$, and as shown by Van Driest[7] a damping factor has to be introduced. Van Driest's analysis can be extended to include transpiration but a large amount of numerical computation is involved and the results are not yet available, though it is hoped to publish them later. An approximate method of predicting the variation of λ with suction or injection is described in Section 4.

2.4. *Experimental Verification of Bilogarithmic Law.*

2.4.1. *Experimental data.*—There exists only a limited amount of experimental data on the velocity distribution in the turbulent boundary layer with suction or injection applied normally through the surface. Some of the available velocity profiles are based on only a few experimental points and therefore cannot provide a conclusive test for any theory, but are included in the present report for completeness.

Twenty-four velocity profiles have been examined, sixteen obtained with suction and eight with injection. All these measurements were obtained with zero pressure gradient, and cover a wide range of suction and injection velocity ratios, as shown in Table 2.4.1.

TABLE 2.4.1

Investigator	Reference	Condition	v_0/U_1	Surface Type	Figure
Sarnecki	Unpublished	Suction	−0·0042	A	2
		Suction	−0·0055	A	2
		Suction	−0·0069	A	2
		Suction	−0·00193	B	3
		Suction	−0·00445	B	3
Dutton	2	Suction	−0·00403	B	4
		Suction	−0·0105	B	4
		Suction	−0·00443	B	5
		Suction	−0·0073	A	5
Kay	1	Suction	−0·00149	C	6
		Suction	−0·00332	C	6
Black	Unpublished	Suction	−0·00809	D	7
		Suction	−0·01075	D	7
		Suction	−0·0213	D	7
		Suction	−0·00321	E	8
		Suction	−0·00465	E	8
Mickley, Ross, Squyers, and Stewart	8	Injection	+0·00207	F	9
		Injection	+0·00506	F	9
		Injection	+0·0105	F	9
Mickley and Davis	5	Injection	+0·0010	F	10
		Injection	+0·0020	F	10
		Injection	+0·0030	F	10
		Injection	+0·0050	F	10
		Injection	+0·0100	F	10

The types of surface listed in Table 2.4.1 are described below.

TABLE 2.4.2

Surface Type	Description
A	Brass sheet, 0·020 in. thick, with 0·020 in. diameter perforations at 0·020 in. spacings in triangular pattern. 22·7% open area.
B	Surface A covered with calendered nylon.
C	Sintered bronze.
D	Aluminium sheet, 0·028 in. thick, drilled with 0·009 in. diameter holes at 0·10 in. spacings in triangular pattern. 0·64% open area.
E	Surface D covered with one sheet of Ford 428 Mill blotting paper.
F	80-mesh Jellif Lectromesh screen, 0·004 in. thick.

2.4.2. *Analysis of velocity profiles obtained with suction.*—In Figs. 2 to 8 inclusive, velocity profiles obtained with suction are examined in the light of the bilogarithmic law. Fig. a in each case shows a plot of $u/U_1 + Y_s^2$ against Y_s, and includes the authors' choice of straight line to fit the bilogarithmic portion of each profile. The slope and intercept of this straight line yields values of U_τ/U_1 and the profile parameter λ [equations (2.3.11), (2.3.19)]. These values enable the profile to be replotted in the familiar form u/U_τ against log $U_\tau y/\nu$ in Fig. b. This plot has been included to show the curvature of the bilogarithmic portion of each profile, which cannot be satisfactorily accounted for by a linear logarithmic law, particularly at high suction rates. Included in Fig. b are sublayer profiles as predicted by equation (4.1.6). Figs. 2 to 8 will now be discussed in detail.

Fig. 2 shows three profiles obtained at different suction rates on a perforated surface (type A) by Sarnecki. Each of these profiles has a clearly defined linear portion in Fig. 2a, while the pronounced curvature of this region in Fig. 2b shows that a linear logarithmic law cannot apply. In Fig. 2a, the chosen straight lines in the case of the lower suction rates do not cut or touch the parabola $u/U_1 = 1$, indicating that the boundary-layer thickness is decreasing locally. For the highest rate of suction, however, the boundary layer has already reached its asymptotic state at the station considered as indicated by the fact that the chosen straight line is tangential to the parabolic curve. It is of interest to note that the bilogarithmic region in the latter case extends to the edge of the boundary layer. The absence of an 'outer' or 'wake' region appears to be a characteristic of the turbulent asymptotic layer.

Fig. 3 shows two profiles obtained by Sarnecki on a porous surface (type B). The bilogarithmic law provides a good fit to the 'inner' portion of the profiles, although the curvature of this region in Fig. 3b is not sufficient to argue positively in its favour. For the lower suction rate, the chosen straight line in Fig. 3a cuts the parabola $u/U_1 = 1$, indicating that the boundary-layer thickness is increasing, i.e. that the layer is undersucked. The chosen straight line for the higher suction rate is almost tangential to the curve indicating near-asymptotic conditions (again note the diminutive size of the 'wake component').

Fig. 4 shows two profiles obtained by Dutton on the same type of surface (type B). Unfortunately very few experimental points were obtained in each case. However, straight lines can be chosen to fit the bilogarithmic portion in Fig. 4a, and the law provides a good interpretation of this region as shown in Fig. 4b. It can be seen from Fig. 4a that the layers are respectively undersucked and oversucked for the lower and higher suction rates.

Fig. 5 shows the profiles of two asymptotic layers obtained by Dutton on surfaces A and B. In each case the suction rate was uniform and was adjusted until an asymptotic layer was obtained over almost the complete test section. Again very few experimental points were recorded, and the choice of straight lines in Fig. 5a, proved difficult. The selected straight lines are tangential to the parabola $u/U_1 = 1$ indicating the asymptotic nature of the layers.

Dutton obtained values of U_τ/U_1 from the asymptotic form of the momentum equation

$$\left(\frac{U_\tau}{U_1}\right)^2 + \frac{v_0}{U_1} = 0 \qquad (2.4.1)$$

and plotted the profiles as u/U_τ against log $U_\tau y/\nu$. He assumed Kay's linear logarithmic law [equation (2.1.6)], which has already been criticised on theoretical grounds, and drew straight lines through the experimental points. It may well be argued on examination of the experimental points in Fig. 5b that this interpretation provides as good a fit as the bilogarithmic law. However the values

of the mixing-length coefficient given by Kay's analysis are 0·35 and 0·31 for the perforated and nylon surfaces (types A and B) respectively, and as it has already been argued that κ should be independent of the suction rate (Section 2.3.2), the bilogarithmic law appears more attractive in this case.

Fig. 6 shows two profiles obtained by Kay on a porous surface (type C). Owing to the relatively low suction rates, the curvature of the bilogarithmic portion in Fig. 6b is only slight.

The profiles of Fig. 7 were obtained by Black on a drilled surface (type D), with relatively high suction rates. They exhibit a marked degree of curvature in Fig. 7b, which is satisfactorily accounted for by the bilogarithmic law.* It is particularly interesting that the law is found to be valid even in the case of a non-homogeneous surface of extremely small open-area ratio (0·65%). The complete absence of a 'wake component' in each case is also worthy of note.

Fig. 8 shows profiles obtained by Black with the drilled sheet covered with a sheet of blotting paper (surface type E). (The blotting paper was used to obtain a more nearly uniform distribution of suction.)

The experimental velocity profiles examined above show satisfactory agreement with the proposed bilogarithmic law, but the boundary-layer growth predicted from the profiles by the present theory can only be checked in two cases apart from that of the asymptotic layers (for which the straight lines are tangent to the parabola as required by the theory). This has been done for the measurements made by Dutton at two suction rates. In each case velocity profiles were measured at close intervals along the test surface, those in Fig. 4 being typical examples. These profiles have been examined by the authors, using the bilogarithmic law to obtain values of U_τ/U_1 from which the growth of momentum thickness has been calculated by means of the momentum equation

$$\frac{d\theta}{dx} = \left(\frac{U_\tau}{U_1}\right)^2 + \frac{v_0}{U_1}. \tag{2.4.2}$$

The calculated and experimental growths of θ are compared in Fig. 9. The remarkably good agreement confirms the values of U_τ/U_1 deduced using the bilogarithmic law. [It should be noted that the two terms on the right-hand side of equation (2.4.2), which are of opposite sign in this case, were of comparable magnitude, so that the measure of agreement obtained becomes even more satisfactory.]

2.4.3. *Analysis of velocity profiles obtained with injection.*—In Figs. 10 and 11, velocity profiles obtained with injection through a mesh surface by Mickley *et al*[8, 5] are examined.

Mickley[8] measured velocity profiles at various stations along the test surface under conditions of suction and injection, with and without heat transfer from the wall.† It was subsequently discovered that the heating cloth, initially attached to the back of the test surface for use in the heat transfer experiments, became detached from it at some stage, permitting longitudinal flow beneath the surface. It was stated by Mickley that, as a result, the reported skin-friction coefficients were likely to be 15 to 30% higher than the correct values, and that in general the results should not be used. Presumably because of the absence of other experimental data, Clarke, Menkes and Libby[3] used three of these profiles to compare with their analysis of the turbulent boundary layer with injection. The agreement they obtained was poor however, particularly in the shape of the profiles, and it was

* The predicted sublayer profiles are included in this figure even though no agreement with the experimental sublayer profiles can be expected in view of the highly non-homogeneous nature of the surface.

† The profiles included in this report were all obtained without heat transfer.

therefore considered of interest to analyse these profiles according to the present theory. The results are shown in Fig. 10. Fig. 10a contains a plot of $u/U_1 - Y_i^2$ against Y_i, from which values of U_τ/U_1 and λ are obtained as in the case of suction. It will be noted that the chosen straight line for the highest injection rate is tangential to the parabola $u/U_1 = 0$ indicating zero effective wall shear. This prevents the replotting of this profile in the conventional manner (u/U_τ against $U_\tau y/\nu$). The other two profiles, however, are replotted in Fig. 10b, and the bilogarithmic law is seen to fit the experimental points quite well.

Mickley[5] later modified his experimental apparatus to eliminate the undesirable effects experienced in his earlier work, and obtained velocity profiles at various stations for different injection rates. Typical profiles are examined in Fig. 11. In Fig. 11a the chosen straight lines for the two lower injection rates cut the parabola $u/U_1 = 0$, indicating positive wall shear. For the intermediate injection rate, ($v_0/U_1 = 0{\cdot}003$) the straight line is almost tangential to the parabola, indicating negligible wall shear. For the two higher injection rates, the straight line lies outside the parabola, indicating negative effective wall shear. The first two profiles are replotted in the form, u/U_τ against log $U_\tau y/\nu$ in Fig. 11b. The curvature of the bilogarithmic region is small in view of the relatively low injection rates. Again, the profile obtained with $v_0/U_1 = 0{\cdot}003$ cannot be replotted as U_τ/U_1 is negligibly small for this case. For the higher injection rates, U_τ/U_1 is imaginary. The bilogarithmic law for imaginary U_τ/U_1 is given in equation (2.3.21) and the profiles may therefore be replotted in the form u/iU_τ against log $iU_\tau y/\nu$, where $i = \sqrt{-1}$. Fig. 11c shows the profiles plotted in this way. It will be seen that the profile for the highest injection rate displays a high degree of curvature which the bilogarithmic law accounts for very satisfactorily.

Mickley calculated U_τ/U_1 from the momentum equation (2.4.2) and obtained negative values of $(U_\tau/U_1)^2$ for the two higher injection rates. As this required taking the small difference of two large quantities, one of which was obtained by differentiation of experimental results, Mickley stated that these negative values were probably of no significance, adding that the measured velocity profiles showed no evidence of separation. In Section 5 of this report the case of transpiration through non-homogeneous surfaces is considered, and the conclusion drawn from this analysis is that negative values of effective* wall shear may occur at high injection rates on surfaces where the hole dimensions are appreciable. It is suggested that this provides the explanation of the negative values of wall shear discussed above. It is important to note that negative effective wall shear in the present case (i.e. for high injection rates) does not imply negative u near the wall, nor even inflection of the velocity profile† such as occurs near separation on a solid surface. There is, in fact, no reason at all to suspect that the injected layer in zero pressure gradient will ever separate in that sense of the word which implies a general breakdown of the boundary-layer flow with associated 'dead-air' region and backflow.

In Fig. 12, the growth of momentum thickness calculated for the five injection rates, using values of U_τ/U_1 obtained from the bilogarithmic law, in conjunction with the momentum equation (2.4.2), is compared with the actual growth of θ obtained experimentally by Mickley. The agreement is quite good. It must be noted, however, that the contribution of the injection term, v_0/U_1, in

* Effective in the sense that these values satisfy the momentum equation (2.4.2) and the bilogarithmic law.

† Although velocity profiles obtained with high injection rates tend to be doubly reflex roughly midway between the wall and the edge of the layer, this is a characteristic of the blown layer and is not in general indicative of zero or negative wall shear.

equation (2.4.2) is in each case substantially greater than that of $(U_\tau/U_1)^2$ and any errors in the latter quantity are therefore largely suppressed in Fig. 12. Average values of $(U_\tau/U_1)^2$ are listed for each case in Fig. 12 to show the relative importance of the two terms.

Discussion of the experimental values of λ determined for the profiles considered in this report will be postponed to Section 4.3.

2.4.4. *Summary of experimental results.*

(1) The bilogarithmic law adequately predicts the velocity distribution in the wall region outside the sublayer, for the cases examined. In particular, profiles obtained with high transpiration rates amply justify the squared-logarithmic term in the law.

(2) The values of U_τ/U_1 obtained from the bilogarithmic law satisfy the momentum equation in the few cases where experimental data are available for comparison.

(3) The bilogarithmic law appears to be equally valid in cases of effectively negative wall shear (imaginary U_τ).

3. *Coles' Wake Hypothesis Applied to Turbulent Boundary Layers with Transpiration.*

3.1. *Introduction.*

Having established the existence of the bilogarithmic law in the inner region of the turbulent boundary layer with transpiration, an attempt can now be made to analyse the outer region of the layer. Stated briefly, the problem is one of determining, if possible, a universal law associated with the velocity distribution in the outer region. Existing theories developed for the particular case of zero transpiration are examined first, to determine whether they may be extended to include the general case of suction or injection. Two approaches which have been made to the problem in the case of no suction are considered below.

3.2. *Velocity-Defect Law.*

It has been found for constant-pressure layers on a solid surface, that the velocity profiles lie close to a single curve when plotted as $(U_1 - u)/U_\tau$ against y/δ (*see* Fig. 3, Ref. 9).

This relationship, expressed in the form

$$\frac{U_1 - u}{U_\tau} = g\left(\frac{y}{\delta}\right), \tag{3.2.1}$$

is known as the velocity-defect law, and implies downstream similarity of the profile. By assuming the existence of the defect law and of a law of the wall of the form

$$\frac{u}{U_\tau} = f\left(\frac{U_\tau y}{\nu}\right), \tag{3.2.2}$$

Millikan deduced the logarithmic law

$$\frac{u}{U_\tau} = A + B \ln \frac{U_\tau y}{\nu} \tag{3.2.3}$$

as follows:

From (3.2.2)
$$\frac{y}{U_\tau}\frac{\partial u}{\partial y} = \frac{yU_\tau}{\nu} f'\left(\frac{U_\tau y}{\nu}\right), \tag{3.2.4}$$

while from the defect law

$$\frac{y}{U_\tau}\frac{\partial u}{\partial y} = -\frac{y}{\delta} g'\left(\frac{y}{\delta}\right). \tag{3.2.5}$$

The concept of overlap is now introduced. This presupposes a finite region in which the defect and wall laws are simultaneously valid. This requires

$$\frac{yU_\tau}{\nu} f'\left(\frac{yU_\tau}{\nu}\right) = -\frac{y}{\delta} g'\left(\frac{y}{\delta}\right)$$

$$= \frac{y}{U_\tau}\frac{\partial y}{\partial y}$$

$$= \frac{1}{\kappa}. \tag{3.2.6}$$

Then κ is determined by either of the variables y/δ or yU_τ/ν, and since these two variables are formally independent of each other, κ must be a constant.

On integrating (3.2.6) in the overlap region, the logarithmic law

$$\frac{u}{U_\tau} = f\left(\frac{yU_\tau}{\nu}\right)$$

$$= A + \frac{1}{\kappa}\ln\frac{U_\tau y}{\nu}$$

$$= A + B\log\frac{U_\tau y}{\nu} \tag{3.2.7}$$

is obtained.

The above result states that the existence of a logarithmic law in the inner region is an essential condition for the validity of the defect law with overlap.

Examination of experimental velocity profiles obtained in pressure gradients has shown that the function $g(y/\delta)$ in equation (3.2.1) is not a universal function (*see* Fig. 18, Ref. 6). To include the effects of pressure gradient, the velocity-defect law must be expressed in the more general form

$$\frac{U_1 - u}{U_\tau} = g\left(\frac{y}{\delta}, \Pi(x)\right), \tag{3.2.8}$$

where the profile parameter Π in general depends on the pressure gradient.

An equilibrium layer has been defined as one for which Π is constant, the constant-pressure layer being a particular example. Clauser[9] has succeeded in obtaining equilibrium layers in pressure gradients of a special form.

When consideration is given to the general case of layers with transpiration, it is obvious from Millikan's analysis that a velocity-defect law $(U_1-u)/U_\tau = g(y/\delta,\ v_0/U_\tau)$ cannot overlap the bilogarithmic law. The assumption of a defect law of this form would therefore require that the overlap region be replaced by a blending region between the inner and outer portions of the layer. Such a requirement would complicate the physical picture unnecessarily and would not provide a sound basis on which to construct a calculation method for the development of sucked or injected layers. The fact that the defect law is not universal for arbitrary pressure gradients provides further ground for its rejection.

Consideration is now given to a more recent approach to the problem.

3.3. *Coles' Wake Hypothesis.*

On examination of a considerable number of experimental velocity profiles obtained on solid surfaces with and without pressure gradients, Coles[6] found that the velocity profile could be written in the form

$$\frac{u}{U_\tau} = A + \frac{1}{\kappa}\left[\ln\frac{U_\tau y}{\nu} + \Pi(x)w\left(\frac{y}{\delta}\right)\right], \tag{3.3.1}$$

where $w(y/\delta)$ is a function which he assumed common to all two-dimensional incompressible turbulent boundary layers on solid surfaces, and $\Pi(x)$ is a profile parameter chosen so that $w(1) = 2$. It is obvious that $w(y/\delta)$ as defined in equation (3.3.1), cannot be a truly universal function, as the condition of zero velocity gradient at the edge of the boundary layer requires from equation (3.3.1) that

$$\left(\frac{dw}{d(y/\delta)}\right)_{y=\delta} = -\frac{1}{\Pi(x)}. \tag{3.3.2}$$

The departure from universality is, however, confined to the edge of the layer and appears to be unimportant. With this restriction, $w(y/\delta)$ can be accepted as a universal function.

In general $\Pi(x)$ depends on the pressure gradient, but for equilibrium layers Π is constant. In particular for constant pressure layers Π is found experimentally to have the value 0·55.

It should be noted that equation (3.3.1) is equivalent to the general form of the velocity-defect law (3.2.8), since

$$\frac{U_1 - u}{U_\tau} = -\frac{1}{\kappa}\left[\ln\frac{y}{\delta} + \Pi[w - w(1)]\right]. \tag{3.3.3}$$

The advantage of Coles' analysis lies in the fact that the function w remains a universal function of y/δ in non-equilibrium layers whereas $(U_1 - u)/U_\tau$ does not. Coles adopted the term 'wake function' in view of the close resemblance between the experimentally determined $w(y/\delta)$ and measurements made in a plane half-wake or half-jet by Liepmann and Laufer[11]. Coles therefore interprets the boundary-layer flow as the summation of two flows; one a wake-type flow, which he tentatively views as a large-scale mixing process constrained by inertia, and the other a constraint-type flow imposed by the condition of zero velocity at the wall, which he regards as a small-scale mixing process constrained by viscosity. It should be observed that in the inner one-fifth or so of the boundary layer, the wake contribution is negligible and the flow is adequately described by the logarithmic law alone. The summation concept is not therefore at variance with established experimental findings.

Denoting the constraint and wake velocity components by u_c and u_w respectively, equation (3.3.1) may be split into two equations

$$\frac{u_c}{U_\tau} = A + \frac{1}{\kappa}\ln\frac{U_\tau y}{\nu} \tag{3.3.4}$$

and

$$\frac{u_w}{U_\tau} = \frac{1}{\kappa}\Pi(x)w\left(\frac{y}{\delta}\right). \tag{3.3.5}$$

These will be referred to as the constraint and wake equations.

The simplest extension of Coles' hypothesis to layers with suction or injection suggests the general form of the constraint and wake equations to be

$$\frac{u_c}{U_\tau} = \frac{U_\tau}{v_0}(\lambda^2 - 1) + \frac{\lambda}{\kappa}\ln\frac{U_\tau y}{\nu} + \frac{1}{4\kappa^2}\frac{v_0}{U_\tau}\left(\ln\frac{U_\tau y}{\nu}\right)^2 \tag{3.3.6}$$

and

$$\frac{u_w}{U_\tau} = \frac{1}{\kappa}\Pi(x)w\left(\frac{y}{\delta}\right), \tag{3.3.7}$$

where the bilogarithmic law replaces the solid-surface logarithmic law, and the wake equation remains unaltered except in so far as $\Pi(x)$ may now be a function of the transpiration rate as well as pressure gradient. The validity of equation (3.3.7) can easily be checked experimentally.

It appears unrealistic, however, that the magnitude of the wake component u_w at every point in the layer, should be determined by the friction velocity U_τ which represents an influence acting at the wall (i.e. wall shear). On the other hand very convincing experimental evidence is presented in Coles' report in favour of the wake law as stated in equation (3.3.5). This suggests the possibility of replacing U_τ in equation (3.3.7) by a representative velocity which may in general be a function of x and y, but which is a constant multiple of U_τ in the particular case of zero transpiration. One such velocity is the local constraint shear velocity u_{*c} defined by

$$u_{*c} = y\frac{\partial u_c}{\partial y}$$

$$= \frac{1}{\kappa}\sqrt{(U_\tau^2 + v_0 u_c)}, \qquad (\textit{see} \text{ Section 6.1})$$

or from equation (3.3.6)

$$u_{*c} = \frac{U_\tau}{\kappa}\left(\lambda + \frac{1}{2\kappa}\frac{v_0}{U_\tau}\ln\frac{U_\tau y}{\nu}\right). \tag{3.3.8}$$

u_{*c} obviously satisfies the two requirements mentioned above; firstly it is a truly local property of the layer, i.e. a function of x and y, and secondly, for zero transpiration ($v_0 = 0$, $\lambda = 1$) it is a constant multiple of U_τ.

On replacing U_τ by u_{*c} equation (3.3.7) becomes

$$\frac{u_w}{u_{*c}} = \Pi(x)w\left(\frac{y}{\delta}\right) \tag{3.3.9}$$

which reduces to equation (3.3.5) for $v_0 = 0$.

u_{*c} increases with y for injection and decreases for suction, but the total variation in u_{*c} across the layer only becomes appreciable at relatively high transpiration rates. It remains, now, to test the validity of equations (3.3.7) and (3.3.9) for the experimental profiles available.

3.4. *Experimental Verification of Coles' Wake Hypothesis for Transpiration Layers.*

Only six of the profiles obtained with suction together with the eight obtained with injection, possessed wake components of sufficient magnitude to permit analysis. In each case the wake component velocity u_w was obtained by subtracting the constraint velocity u_c (as determined from the

bilogarithmic law) from the total velocity u. Equations (3.3.6) and (3.3.8) were then applied to obtain Π_τ, w_τ (y/δ) and Π_*, w_* (y/δ) respectively†, δ being determined by the maximum value of u_w/U_τ or u_w/u^*_c. w_τ and w^* were then obtained by satisfying Coles' normalising condition $w(1) = 2$, while Π followed from the equations

$$\Pi_\tau = \left(\frac{\kappa u_w}{2U_\tau}\right)_{y=\delta} \tag{3.4.1}$$

and

$$\Pi_* = \left(\frac{u_w}{2u_{*c}}\right)_{y=\delta}. \tag{3.4.2}$$

w_τ and w^* are plotted for each of the profiles considered in sub-figures a and b of Figs. 14 to 18. Included in each figure is the wake function as tabulated by Coles.

Fig. 14 shows the functions w_τ and w_* obtained from two of the velocity profiles of Fig. 2. The agreement between w_τ and Coles' Wake Function is poor. The agreement for w_*, although considerably better, is still not of the standard obtained by Coles for the solid-surface data. The profiles in question, however, were obtained in oversucked layers. In such layers the value of u_{*c} decreases rapidly with increasing y to approximately zero at the edge of the boundary layer, and accurate determination of δ and $w(y/\delta)$ becomes exceedingly difficult.

The functions w_τ and w_* for the suction profiles shown in Fig. 3 are plotted in Fig. 15. Agreement with the Wake Function is fair for w_τ but good for w_* within the experimental scatter.‡

w_τ and w_* for the profiles of Fig. 8 are plotted in Fig. 16. Again the agreement, whilst only fair for w_τ, is good for w_*.

In Figs. 17 and 18, w_τ and w_* are plotted for the injection profiles of Figs. 9 and 10. Here again the experimental evidence appears to be slightly in favour of w_* which agrees well with the Wake Function.

In each of Figs. 14 to 18, values of Π_τ and Π_* are included. Both Π_τ and Π_* tend to decrease with increasing suction, and increase with increasing injection, although this trend is not well defined. In particular, imaginary values of Π_τ are obtained for two of the injection cases in Fig. 18. These values occur as a direct consequence of the non-homogeneity of the surface, which results in negative effective wall shear (imaginary U_τ). (See Section 5.) It is unlikely, however, that the flow in the outer region should be directly affected by non-homogeneity of the surface, and it appears unrealistic, therefore, that the wake parameter should be so intimately associated with the surface condition. This adds emphasis to the argument previously advanced in favour of using u_{*c} as the representative velocity in the wake.

No conclusions can safely be drawn from the values of Π regarding the equilibrium of constant-pressure transpiration layers, for it must be remembered that u_{*c}, while being perhaps the most obvious, is not the only representative velocity satisfying the requirements discussed earlier, and that the choice of some suitable alternative would in general result in different experimental values of Π.

---

† Π_τ, Π_*, w_τ, w_* are used to distinguish between experimental profiles plotted according to equations (3.3.7) and (3.3.9).

‡ It should be noted that experimental errors in the original velocity distribution are considerably magnified in the plot of $w(y/\delta)$.

3.5. *Summary.*

(i) The possibility of describing the flow in the outer region of turbulent boundary layers with transpiration in terms of the velocity-defect law has been rejected, principally because of incompatibility with the bilogarithmic law when overlap is assumed.

(ii) From a study of the limited experimental evidence available, it is concluded that the wake hypothesis developed by Coles for layers on solid surfaces remains valid in layers with transpiration.

(iii) In extending Coles' hypothesis to include transpiration the question arises concerning the correct representative velocity with which to describe the wake flow. It is suggested that the use of u_{*c} is more consistent with the physical picture of the basic flow mechanism provided by the hypothesis. In the particular case of zero transpiration, $u_{*c} = (1/\kappa)U_\tau$ and the wake equation reduces to the form given by Coles for layers on solid surfaces. The experimental evidence, although not conclusive, appears to favour the use of u_{*c}.

4. *The Wall Boundary Condition in Two-dimensional Flow.*

4.1. *The Sublayer and Blending Region.*

In a two-dimensional turbulent boundary layer on a solid surface at very small distance from the surface the turbulent shear $\langle -u'v' \rangle$ is small compared with the viscous shear $\nu\,\partial u/\partial y$, so that the flow behaves as though it were laminar.

If the surface is smooth, the flow in the sublayer is two-dimensional and described adequately by equation (2.2.5a) in which

$$\frac{\tau}{\rho} = \nu \frac{\partial u}{\partial y},$$

so that

$$\nu \frac{\partial u}{\partial y} = \text{const.} = \left(\nu \frac{\partial u}{\partial y}\right)_{y=0} = U_\tau^2, \tag{4.1.1}$$

and so

$$u = \frac{U_\tau^2 y}{\nu}, \quad \text{or} \quad \frac{u}{U_\tau} = \frac{U_\tau y}{\nu}. \tag{4.1.2}$$

If the surface is permeable, but nevertheless smooth and homogeneous, the basic relationships are unchanged, but the transpiration velocity must be taken into account, so that equation (2.2.5a) has to be replaced by the more general form of equation (2.2.5), which leads to the velocity-shear relationship, (2.2.8)

$$U_\tau^2 + v_0 u = \frac{\tau}{\rho} = \nu \frac{\partial u}{\partial y} = \frac{\nu}{v_0} \frac{\partial}{\partial y}(U_\tau^2 + v_0 u). \tag{4.1.3}$$

Hence

$$U_\tau^2 + v_0 u = U_\tau^2\, e^{v_0 y/\nu}, \tag{4.1.4}$$

or

$$\frac{u}{v_0} = \frac{U_\tau^2}{v_0^2}(e^{v_0 y/\nu} - 1), \tag{4.1.5}$$

or

$$\frac{u}{U_\tau} = \frac{U_\tau}{v_0}(e^{v_0 y/\nu} - 1), \tag{4.1.6}$$

or

$$\frac{u}{U_1} = \frac{U_\tau^2}{v_0 U_1}(e^{v_0 U_1 \cdot U_1 y/\nu} - 1). \tag{4.1.7}$$

Between the sublayer and the fully turbulent régime there is a blending region in which the viscous and turbulent stresses are of comparable magnitude. This region has been largely neglected in the past, since any theory describing it must rely mainly on empirical data, whilst the effect of the flow in this region on the rest of the layer is confined to the value of the constant A in the turbulent wall law, (2.3.3a). This constant can be determined empirically more easily than the flow in the narrow blending region. For the purposes of evaluating such flow quantities as displacement or momentum thickness sufficient accuracy is obtained by assuming the laws of the sublayer and of the turbulent régime to hold on either side of a 'transition point', $y = y_a$ at which the velocities given by the two laws are equal.

A theory for the flow in the blending region of a solid boundary layer has been put forward by Van Driest[7], and it is hoped to extend this to layers with transpiration in a future paper. For the present the 'transition point' approach will be used.

The predicted sublayer profiles are plotted in each of the figures showing the experimental velocity distributions. It is seen that agreement is generally poor, but this can be ascribed to

(i) the inevitably large percentage error in the measurement of small wall distances,

(ii) the unreliability of pitot-tube readings in the immediate vicinity of the wall (no corrections have been applied),

(iii) non-homogeneity effects (*see* Section 5).

4.2. *The Transition Point.*

The '*transition point*' $y = y_a$ is given by the sublayer and bilogarithmic laws, equations (4.1.4), (2.2.17):

$$U_\tau^2 + v_0 u_a = \left(\frac{v_0}{2\kappa} \ln \frac{y_a}{d}\right)^2 = U_\tau^2 \, e^{v_0 y_a/\nu},$$

so that

$$e^{v_0 y_a/\nu} = \left(\frac{1}{2\kappa} \frac{v_0}{U_\tau} \ln \frac{y_a}{d}\right)^2. \tag{4.2.1}$$

It has been shown [cf. (2.2.18)] that $v_0 \ln y/d > 0$ throughout the bilogarithmic region, so that

$$e^{\frac{1}{2}v_0 y_a/\nu} = \frac{1}{2\kappa} \frac{v_0}{U_\tau} \ln \frac{y_a}{d}. \tag{4.2.2}$$

This is the equation relating y_a and d for given v_0, U_τ and κ. It can be rewritten as

$$e^{\frac{1}{2}v_0 y_a/\nu} = \frac{1}{2\kappa} \frac{v_0}{U_\tau} \left(\ln \frac{U_\tau y_a}{\nu} - \ln \frac{U_\tau d}{\nu}\right)$$

$$= \frac{1}{2\kappa} \frac{v_0}{U_\tau} \ln \frac{U_\tau y_a}{\nu} + \lambda, \tag{4.2.3}$$

in view of (2.3.5). The velocity u_a at $y = y_a$ is

$$u_a = \frac{U_\tau^2}{v_0} (e^{v_0 y_a/\nu} - 1), \tag{4.2.4}$$

whilst the velocity gradients at $y = y_a$ given by the two laws are

$$\left(\frac{\partial u}{\partial y}\right)_a = \frac{U_\tau^2}{\nu} e^{v_0 y_a/\nu} \qquad \text{(sublayer)} \qquad (4.2.5)$$

and

$$\left(\frac{\partial u}{\partial y}\right)_a = \frac{1}{\kappa y_a}\left(\frac{v_0}{2\kappa}\ln\frac{y_a}{d}\right) = \frac{U_\tau}{\kappa y_a} e^{\frac{1}{2}v_0 y_a/\nu} \text{ (bilogarithmic)}, \qquad (4.2.6)$$

in view of (4.2.2).

In the case of solid boundaries the relationship between u/U_τ and $U_\tau y/\nu$ in the wall region is unique; in particular both the sublayer and turbulent laws are of the form $u/U_\tau = f(U_\tau y/\nu)$, hence at their intersection the values of (u/U_τ), $(U_\tau y/\nu)$, $\partial(u/U_\tau)/\partial(U_\tau y/\nu)$ and higher derivatives are all uniquely defined, viz. if N is given by

$$N = A + \frac{1}{\kappa}\ln N, \qquad (4.2.7)$$

then

$$\frac{u_a}{U_\tau} = N; \quad u_a = NU_\tau \qquad (4.2.8)$$

$$\frac{U_\tau y_a}{\nu} = N; \quad y_a = N\frac{\nu}{U_\tau} \qquad (4.2.9)$$

$$\partial\left(\frac{u}{U_\tau}\right)\Big/\partial\left(\frac{U_\tau y}{\nu}\right) = 1 \text{ at } y_a; \quad \left(\frac{\partial u}{\partial y}\right)_a = \frac{U_\tau^2}{\nu} \qquad \text{(sublayer)} \qquad (4.2.10)$$

$$\partial\left(\frac{u}{U_\tau}\right)\Big/\partial\left(\frac{U_\tau y}{\nu}\right) = \frac{1}{\kappa N} \text{ at } y_a; \quad \left(\frac{\partial u}{\partial y}\right)_a = \frac{U_\tau^2}{\kappa N \nu} \qquad \text{(turbulent)}. \qquad (4.2.11)$$

4.3. *Transition Criteria.*

The transition point determines a number of dimensionless quantities, each of them in effect a 'critical Reynolds number'. It is therefore of interest to use this superficial analogy with the conventional transition from laminar to turbulent flow in a boundary layer or a channel in order to develop a theory for the variation of the distance y_a (and hence the parameter λ in the bilogarithmic law) with changing suction or injection velocity. Thus the hypothesis is made that there exists a single criterion which determines the transition point at *all* values of v_0, provided the surface is smooth and homogeneous so that no disturbances are introduced by the transpiration (cf. Section 5). This criterion will involve the achievement of a critical value by some dimensionless parameter, this critical value being independent of v_0.

Almost any combination of (u/U_τ), $(U_\tau y/\nu)$ and their mutual derivatives can provide a possible criterion, since they all have unique values at $y = y_a$ in the case of solid boundaries, though these values may (*a priori*) vary with v_0, so that the choice of the right parameter must be determined experimentally, by comparing the observed values of λ with those predicted by each particular criterion.

The simplest quantities which might be combined to provide the required parameters are $(U_\tau y/\nu)$, (u/U_τ) and $\partial(u/U_\tau)/\partial(U_\tau y/\nu)$: ($v_0$, whilst entering implicitly through the sublayer and bilogarithmic

laws may be assumed not to enter explicitly as it vanishes in the solid case). Their most obvious combinations (and corresponding critical values for $v_0 = 0$) are shown in Table 4.3.1.*

TABLE 4.3.1

Possible Transition Criteria

Quantity	Behaviour with increasing y for $v_0 = 0$	Value at $y = y_a$ for $v_0 = 0$
$\frac{U_\tau y}{\nu}$	increasing	N (i)
$\frac{u}{U_\tau}$	increasing	N (ii)
$\frac{uy}{\nu} = \left(\frac{u}{U_\tau}\right)\left(\frac{U_\tau y}{\nu}\right)$	increasing	N^2 (iii)
$\frac{y^2}{\nu}\frac{\partial u}{\partial y} = \left(\frac{U_\tau y}{\nu}\right)^2 \frac{\partial(u/U_\tau)}{\partial(U_\tau y/\nu)}$	increasing increasing	N^2 in the sublayer law (iv) N/κ in the turbulent law (v)
$\frac{y}{U_\tau}\frac{\partial u}{\partial y} = \left(\frac{U_\tau y}{\nu}\right) \frac{\partial(u/U_\tau)}{\partial(U_\tau y/\nu)}$	increasing constant	N in the sublayer law (vi) $1/\kappa$ in the turbulent law (vii)
$\frac{u}{y\frac{\partial u}{\partial y}} = \frac{(u/U_\tau)}{\left(\frac{U_\tau y}{\nu}\right)\frac{\partial(u/U_\tau)}{\partial(U_\tau y/\nu)}}$	constant increasing	1 in the sublayer law (viii) κN in the turbulent law (ix)
$\frac{U_\tau^2}{\nu\frac{\partial u}{\partial y}} = \frac{1}{\frac{\partial(u/U_\tau)}{\partial(U_\tau y/\nu)}}$	constant increasing	1 in the sublayer law (x) κN in the turbulent law (xi)
$\frac{u^2}{\nu\frac{\partial u}{\partial y}} = \frac{(u/U_\tau)}{\frac{\partial(u/U_\tau)}{\partial(U_\tau y/\nu)}}$	increasing increasing	N^2 in the sublayer law (xii) κN^3 in the turbulent law (xiii)

Each of the above parameters (except those which are constant for $v_0 = 0$) will now be treated as a possible 'transition criterion' and the corresponding variation of λ examined.

* It must be stressed that the supposed existence of a transition criterion is a hypothesis deduced by analogy from the observed behaviour of turbulent boundary layers on solid walls and is *not* a basic *physical* truth; consequently no physical argument can determine which particular criterion will give the best agreement with experimental results. This could only be achieved by a theory describing in detail the flow in the blending region. As it is, only approximate agreement between predicted and actual variation of λ can be expected, so that simplicity of the criterion and its application is desirable. Thus, although the total number of possible criteria is infinite, only those listed above need be examined.

For each of the criteria listed in Table 4.3.1 the value of y_a in terms of U_τ, v_0, etc., is determined through equations (4.2.4) to (4.2.6). λ is then obtained from (4.2.3).

To simplify the calculations, v_0/U_τ is replaced by the quantity $(N/2)(v_0/U_\tau)$ and $(1/N)(U_\tau y_a/\nu)$ is used as a non-dimensional form of the 'sublayer thickness' y_a. The following notation will be used:

$$\frac{N}{2}\frac{v_0}{U_\tau} = m, \tag{4.3.1}$$

$$\frac{1}{N}\frac{U_\tau y_a}{\nu} = n. \tag{4.3.2}$$

when $v_0 = 0$, $m = 0$, $n = 1$.

In some cases it is convenient to use B instead of $1/\kappa$ (cf. Appendix II).

Thus

$$\frac{1}{2}\frac{v_0 y_a}{\nu} = mn, \tag{4.3.3}$$

$$\frac{1}{2\kappa}\frac{v_0}{U_\tau} = \frac{B}{N}m, \tag{4.3.4}$$

and equations (4.2.4) to (4.2.6) become

$$u_a = U_\tau \frac{N}{2m}(e^{2mn}-1), \tag{4.3.5}$$

$$\left(\frac{\partial u}{\partial y}\right)_a = \frac{U_\tau^2}{\nu} e^{2mn} \text{ in the sublayer law,} \tag{4.3.6}$$

$$\left(\frac{\partial u}{\partial y}\right)_a = \frac{U_\tau^2}{\nu}\frac{1}{\kappa Nn} e^{mn} \text{ in the turbulent law,} \tag{4.3.7}$$

whilst

$$y_a = \frac{\nu}{U_\tau} Nn. \tag{4.3.8}$$

Finally equation (4.2.3) becomes

$$\lambda = e^{mn} - m\frac{B}{N}\log Nn. \tag{4.3.9}$$

The details of the calculations can be found in Appendix III. The results are summarised in Table 4.3.2.

The quantities marked (vii), (viii) and (x) in Table 4.3.1 are constant throughout the layer when $v_0 = 0$ and therefore cannot serve as transition criteria.

All the above functions λ have been computed for a wide range of values of v_0/U_τ, with particular emphasis on negative values (suction) for which more experimental data are available. The constants used were (*see* Appendix I)

$$N = 11{\cdot}2, \quad A = 5{\cdot}4, \quad B_{10} = 5{\cdot}5, \quad B_c = 2{\cdot}39, \quad \kappa = 0{\cdot}419.$$

The numerical values of λ are shown in Table III.1 and plotted in Fig. 13a. The curve of λ against v_0/U_τ predicted by criterion (ii), $u_a/U_\tau = N$ is replotted in Fig. 13b together with experimental results. This particular criterion was chosen as it appears to predict most accurately the actual variation of λ for layers on smooth, nearly homogeneous walls. Also this criterion predicts a maximum suction rate above which the basic assumptions regarding the transition-point break

TABLE 4.3.2

Variation of λ with v_0/U_τ as predicted by Various Transition Criteria

Criterion	Variation of λ with v_0/U_τ	Remarks
(i) $\dfrac{U_\tau y}{\nu} = N$	$\lambda = e^m - m\dfrac{B}{N}\log N$	
(ii) $\dfrac{u}{U_\tau} = N$	$\lambda = \frac{1}{2}(1+2m) - m\dfrac{B}{N}\log\left\{\dfrac{\ln(1+2m)}{2m}\right\} - m\dfrac{B}{N}\log N$	$m > -\frac{1}{2}$
(iii) $\dfrac{uy}{\nu} = N^2$	$\lambda = e^{x(m)} - m\dfrac{B}{N}\log\dfrac{x(m)}{m} - m\dfrac{B}{N}\log N$	$x(t)$ defined by $xe^x \sinh x = t^2$
(iv) $\dfrac{y^2}{\nu}\dfrac{\partial u}{\partial y} = N^2$ in the turbulent law	$\lambda = e^{y(m)} + \dfrac{m}{\kappa N}y(m) - m\dfrac{B}{N}\log N$	$m > -\dfrac{1}{\rho} = -0{\cdot}368$; $y(t)$ defined by $ye^y = t$
(v) $\dfrac{y^2}{\nu}\dfrac{\partial u}{\partial y} = \dfrac{N}{\kappa}$ in the turbulent law as in (iv)		
(vi) $\dfrac{y}{U_\tau}\dfrac{\partial u}{\partial y} = N$ in the sublayer law	$\lambda = e^{\frac{1}{2}y(2m)} + \dfrac{m}{\kappa N}y(2m) - m\dfrac{B}{N}\log N$	$m > -\dfrac{1}{2\rho} = -0{\cdot}184$; cf. (iv)
(ix) $\dfrac{u}{y\dfrac{\partial u}{\partial y}} = \kappa N$ in the turbulent law	$\lambda = e^{\phi} + m\dfrac{B}{N}\log\dfrac{\sinh\phi}{\phi} - m\dfrac{B}{N}\log N$	$\sinh\phi = m$
(xi) $\dfrac{U_\tau^2}{\nu\dfrac{\partial u}{\partial y}} = \kappa N$ in the turbulent law	$\lambda = e^{-y(-m)} + \dfrac{m}{\kappa N}y(-m) - m\dfrac{B}{N}\log N$	$m < \dfrac{1}{\rho} = 0{\cdot}368$; cf. (iv)
(xii) $\dfrac{u^2}{\nu\dfrac{\partial u}{\partial y}} = N^2$ in the sublayer law as in (ix)		
(xiii) $\dfrac{u^2}{\nu\dfrac{\partial u}{\partial y}} = \kappa N^3$ in the turbulent law	$\lambda = e^{z(m)} - m\dfrac{B}{N}\log\dfrac{z(m)}{m} - m\dfrac{B}{N}\log N$	$z(t)$ defined by $ze^z \sinh^2 z = t^3$

down, as must be the case when a turbulent layer reverts to laminar flow under the influence of strong suction. The critical value of $-v_0/U_\tau = 0{\cdot}089$ appears realistic in view of Dutton's results, viz. a turbulent asymptotic layer [for which $-v_0/U_\tau = \sqrt{(-v_0/U_1)}$] was obtained by him on a smooth nylon surface with $-v_0/U_1 = 0{\cdot}00443$, i.e. $-v_0/U_\tau = 0{\cdot}067$ whereas at $-v_0/U_1 = 0{\cdot}0125$ ($-v_0/U_\tau = 0{\cdot}112$) an initially turbulent layer reverted to a laminar state, quickly reaching asymptotic conditions. Other possible transition criteria [(iv) and (vi)] also predict a critical suction rate, but the predicted variations of λ are not borne out by experiment and the critical rates appear too low.

In (iv) $(-v_0/U_\tau)_{\text{crit}} = 0{\cdot}0657$, in (vi) $(-v_0/U_\tau)_{\text{crit}} = 0{\cdot}0329$, both *lower* than Dutton's observed $0{\cdot}067$ in a fully turbulent asymptotic layer.

Not too much stress should however be laid on the correspondence between critical values of v_0/U_τ in the transition-point analysis and the reversion to laminar flow, as the transition approach is mainly empirical in concept and can only obscure the physical mechanism of the flow which is likely to govern the process of laminar reversion. The absence of a critical suction rate is not therefore a sufficient reason for the rejection of a possible criterion, though its low value for (iv) and (vi) provides a strong argument against their acceptability. The others [except possibly (xi) which predicts a very low critical *blowing* rate] must all remain as 'possibles' until more experimental data on the variation of λ with v_0/U_τ are available. For the present it can only be said that (ii) appears to give the best agreement with experimental results obtained on smooth, nearly homogeneous surfaces.

The values of λ obtained on non-homogeneous (drilled or perforated) surfaces are seen from Fig. 13b to be higher than those on smooth surfaces at the same *suction* rate ($-v_0/U_\tau$). Since the value of λ at $v_0 = 0$ must be unity, the effect of non-homogeneity is to reduce the value of $d\lambda/d(v_0/U_\tau)$ and hence the value of the constant A in the solid-plate logarithmic law, equation (2.3.3a). This is in keeping with the analogy between non-homogeneity and roughness, since the effect of roughness on solid surfaces is to decrease the constant A in the logarithmic law.

5. *Effects of Roughness and Non-Homogeneity of the Wall Surface.*

In the theoretical analysis given earlier, the usual assumption of boundary-layer theory has been made, that the variation of all flow quantities parallel to the boundary $y = 0$ are small compared with the variation normal to the boundary, i.e. for all quantities q

$$\left|\frac{\partial q}{\partial x}\right|, \left|\frac{\partial q}{\partial z}\right| \ll \left|\frac{\partial q}{\partial y}\right|.$$

This condition holds for what may be termed a homogeneous boundary layer, i.e. a layer on a smooth surface with no discrete orifices. When transpiration is applied, however, the surface is never homogeneous since the in- or out-flow takes place through discrete holes or pores and the theoretical boundary $y = 0$ consists of both solid area (where locally $u_0 = v_0 = 0$) and open area where $v_0 \neq 0$ and probably $u_0 \neq 0$. In this section the equations of motion are considered for the case where, in addition to the gradual overall variation of flow quantities along the boundary, there is a fairly large spatial fluctuation about the overall mean values due to the presence of a discontinuous boundary.

The spatial fluctuations are confined to a region near the boundary: the thickness of their region of influence must depend primarily on the size and spacing of the orifices, when the mean flow velocities and open-area ratio are kept constant. In particular the fluctuation region must become

thinner when the hole size is decreased. Thus on a coarse perforated plate this region will be thicker than on a fine gauze with the same open area. Using a sufficiently fine surface the fluctuation region may be made to occupy only a small proportion of the boundary-layer thickness. When the spatial fluctuations are confined to the sublayer it can be expected that their presence will not affect the flow at larger distances from the surface. Thus the surface will be effectively homogeneous, just as a solid surface is aerodynamically smooth if the roughness elements are all embedded in the sublayer. The two cases are not entirely analogous, however, since the thickness of the fluctuation region in a transpiration layer depends not only on U_τ and ν but also on v_0.

It must be the aim of any boundary-layer theory to provide a basis for the prediction of boundary-layer growth in the conditions considered. In the case of the turbulent layer with transpiration the first step is the theory of the velocity profile, such as that considered in this report. The next step must be to find the way in which a boundary layer grows at different rates of suction and injection on an effectively homogeneous surface, since the development of the layer on a non-homogeneous surface must depend also on the extent of non-homogeneity. (Thus, starting from the same initial conditions, asymptotic boundary layers of the same thickness are obtained at different rates of suction on different types of surfaces (Dutton[2]). It is also necessary to find a criterion for homogeneity of surface, so that a development theory may be compared with experimental results obtained in conditions which are effectively homogeneous. Experimentation to this end is needed before such a criterion can be found.

The Navier-Stokes equation considers the momentum balance in a control volume

$$\frac{\partial}{\partial t}(\rho u_i) + \frac{\partial}{\partial x_j}(\rho u_i u_j) = -\frac{\partial p}{\partial x_i} + \frac{\partial}{\partial x_j}\left[\mu\left(\frac{\partial u_i}{\partial x_j} + \frac{\partial u_j}{\partial x_i}\right)\right] \tag{5.1}$$

$$\left[\begin{matrix}\text{Momentum growth}\\ \text{with time}\end{matrix}\right] + \left[\begin{matrix}\text{Flux}\\ \text{of momentum}\end{matrix}\right] = \left[\begin{matrix}\text{Pressure}\\ \text{force}\end{matrix}\right] + \left[\begin{matrix}\text{Viscous}\\ \text{force}\end{matrix}\right].$$

In a uniform incompressible fluid ρ, μ are constants and the continuity equation takes the form

$$\frac{\partial u_j}{\partial x_j} = 0. \tag{5.2}$$

When mean values are taken in any way whatever (i.e. with respect to time or space), so that

$$q = \langle q\rangle \text{ (mean)} + q' \text{ (fluctuating value)} \tag{5.3}$$

then

$$\langle q_1 q_2\rangle = \langle\langle q_1\rangle\langle q_2\rangle + \langle q_1\rangle q_2' + q_1'\langle q_2\rangle + q_1' q_2'\rangle = \langle q_1\rangle\langle q_2\rangle + \langle q_1' q_2'\rangle, \tag{5.4}$$

since

$$\langle q'\rangle = 0.$$

The mean value expressions for (5.1) and (5.2) can therefore be written

$$\rho\frac{\partial}{\partial t}\langle u_i\rangle + \rho\frac{\partial}{\partial x_j}\langle u_i\rangle\langle u_j\rangle = -\frac{\partial}{\partial x_i}\langle p\rangle + \frac{\partial}{\partial x_j}\left[\mu\left(\frac{\partial\langle u_i\rangle}{\partial x_j} + \frac{\partial\langle u_j\rangle}{\partial x_i}\right) - \rho\langle u_i' u_j'\rangle\right], \tag{5.5}$$

$$\frac{\partial\langle u_j\rangle}{\partial x_j} = 0 \text{ and also } \frac{\partial u_j'}{\partial x_j} = 0. \tag{5.6}$$

If the flow is steady-turbulent and also the x- and z-wise variation can be resolved into a slow overall variation and a rapid local fluctuation (cf. Fig. 5.1) with zero mean value, then any q can be subdivided as follows:

$$q = \langle q \rangle + q' = \{q\} + q^x = \{\langle q \rangle\} + \{q'\} + \langle q^x \rangle + q'^x, \tag{5.7}$$

where $\langle\ \rangle$ is time mean, $\{\}$ is space mean.

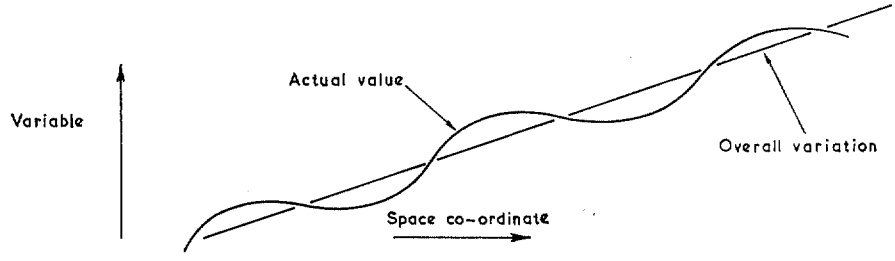

FIG. 5.1. Illustrating the two modes of spatial variation.

Under the conditions of the problem $(\partial/\partial t)\langle q \rangle = 0$, but $(\partial/\partial x_i)\{q\}$ need not vanish even for $x_i = x$ or z. Taking the double mean of (5.1) and noting that

$$\{\langle q_1 q_2 \rangle\} = \{\langle q_1 \rangle\}\{\langle q_2 \rangle\} + \langle\{q_1'\}\{q_2'\}\rangle + \{\langle q_1^x \rangle \langle q_2^x \rangle\} + \{\langle q_1'^x q_2'^x \rangle\}, \tag{5.8}$$

$$\rho \frac{\partial}{\partial x_j}\{\langle u_i \rangle\}\{\langle u_j \rangle\} = -\frac{\partial}{\partial x_i}\{\langle p \rangle\} + \frac{\partial}{\partial x_j}\left[\mu\left(\frac{\partial}{\partial x_j}\{\langle u_i \rangle\} + \frac{\partial}{\partial x_i}\{\langle u_j \rangle\}\right) - \rho\langle\{u_i'\}\{u_j'\}\rangle - \right.$$

$$\left. - \rho\{\langle u_i^x \rangle \langle u_j^x \rangle\} - \rho\{\langle u_i'^x u_j'^x \rangle\}\right], \tag{5.9}$$

i.e.

$$\rho \frac{\partial}{\partial x_j}\{\langle u_i \rangle\}\{\langle u_j \rangle\} = -\frac{\partial}{\partial x_i}\{\langle p \rangle\} + \frac{\partial}{\partial x_j}\sigma_{ij}, \tag{5.10}$$

with

$$\sigma_{ij} = \mu\left[\frac{\partial}{\partial x_j}\{\langle u_i \rangle\} + \frac{\partial}{\partial x_i}\{\langle u_j \rangle\}\right] + [-\rho\langle\{u_i'\}\{u_j'\}\rangle] + [-\rho\{\langle u_i'^x u_j'^x \rangle\}] + [-\rho\{\langle u_i^x \rangle\langle u_j^x \rangle\}]$$

(effective shear stress) (viscous stress) (Reynolds stress) (spatial fluctuation stress). (5.11)

If the overall flow is two-dimensional, $(\partial/\partial z)\{\langle q \rangle\} = 0$, then

$$\left.\begin{aligned} \rho \frac{\partial}{\partial x}\{\langle u^2 \rangle\} + \rho \frac{\partial}{\partial y}\{\langle u \rangle\}\{\langle v \rangle\} &= -\frac{\partial}{\partial x}\{\langle p \rangle\} + \left[\frac{\partial}{\partial x}\sigma_{xx} + \frac{\partial}{\partial y}\sigma_{xy}\right], \\ \rho \frac{\partial}{\partial x}\{\langle u \rangle\}\{\langle v \rangle\} + \rho \frac{\partial}{\partial y}\{\langle v^2 \rangle\} &= -\frac{\partial}{\partial y}\{\langle p \rangle\} + \left[\frac{\partial}{\partial x}\sigma_{xy} + \frac{\partial}{\partial y}\sigma_{yy}\right], \end{aligned}\right\} \tag{5.12}$$

$$\frac{\partial\{\langle u \rangle\}}{\partial x} + \frac{\partial\{\langle v \rangle\}}{\partial y} = 0. \tag{5.13}$$

Now the x-variation of the double mean is slight, $|\partial/\partial x\{\langle q\rangle\}| \ll |\partial/\partial y\{\langle q\rangle\}|$ so that the Prandtl approximation can be applied as to a two-dimensional boundary layer.

$$\frac{\partial\{\langle p\rangle\}}{\partial y} = 0, \tag{5.14}$$

$$\{\langle u\rangle\}\frac{\partial\{\langle u\rangle\}}{\partial x} + \{\langle v\rangle\}\frac{\partial\{\langle u\rangle\}}{\partial y} = -\frac{1}{\rho}\frac{d}{dx}\{\langle p\rangle\} + \frac{1}{\rho}\frac{\partial}{\partial y}\sigma, \tag{5.15}$$

$$\sigma = \mu\frac{\partial}{\partial y}\{\langle u\rangle\} - \rho\langle\{u'\}\{v'\}\rangle - \rho\{\langle u'^x v'^x\rangle\} - \rho\{\langle u^x\rangle\langle v^x\rangle\}. \tag{5.16}$$

Equation (5.15) can be integrated between $y = 0$ and $y = \delta$ (edge of the boundary layer) using $U_1\, dU_1/dx = -1/\rho\, d/dx\{\langle p\rangle\}$ and writing

$$\int_0^\delta (U_1 - \{\langle u\rangle\})\,dy = U_1\delta^*, \quad \int_0^\delta \{\langle u\rangle\}(U_1 - \{\langle u\rangle\})\,dy = U_1^2\theta.$$

Then

$$\begin{aligned}
\frac{d}{dx}(U_1^2\theta) &= \int_0^\delta \frac{\partial}{\partial x}[\{\langle u\rangle\}(U_1 - \{\langle u\rangle\})]\,dy \\
&= U_1\int_0^\delta \frac{\partial\{\langle u\rangle\}}{\partial x}\,dy + \frac{dU_1}{dx}\int_0^\delta \{\langle u\rangle\}\,dy - 2\int_0^\delta \{\langle u\rangle\}\frac{\partial\{\langle u\rangle\}}{dx}\,dy \\
&= U_1\int_0^\delta \frac{\partial\{\langle u\rangle\}}{\partial x}\,dy + \frac{dU_1}{dx}\int_0^\delta \{\langle u\rangle\}\,dy - \int_0^\delta \{\langle u\rangle\}\frac{\partial\{\langle u\rangle\}}{dx}\,dy + \Big[\{\langle u\rangle\}\{\langle v\rangle\}\Big]_0^\delta - \\
&\quad - \int_0^\delta \{\langle v\rangle\}\frac{\partial\{\langle u\rangle\}}{\partial y}\,dy \\
&= U_1\left[\int_0^\delta \frac{\partial\{\langle u\rangle\}}{\partial x}\,dy + \{\langle v_\delta\rangle\}\right] - \{\langle u_0\rangle\}\{\langle v_0\rangle\} + \frac{dU_1}{dx}\int_0^\delta \{\langle u\rangle\}\,dy - \\
&\quad - \int_0^\delta \left(\{\langle u\rangle\}\frac{\partial\{\langle u\rangle\}}{\partial x} + \{\langle v\rangle\}\frac{\partial\{\langle u\rangle\}}{dy}\right)dy \\
&= U_1\{\langle v_0\rangle\} - \{\langle u_0\rangle\}\{\langle v_0\rangle\} + \frac{dU_1}{dx}\int_0^\delta \{\langle u\rangle\}\,dy - \int_0^\delta \left(U_1\frac{dU_1}{dx} + \frac{1}{\rho}\frac{\partial\sigma}{\partial y}\right)dy \\
&= U_1\{\langle v_0\rangle\} - \{\langle u_0\rangle\}\{\langle v_0\rangle\} + \frac{dU_1}{dx}\int_0^\delta (\{\langle u\rangle\} - U_1)\,dy + \frac{\sigma_0}{\rho},
\end{aligned}$$

i.e.

$$\frac{d}{dx}(U_1^2\theta) + \frac{dU_1}{dx}U_1\delta^* = U_1\{\langle v_0\rangle\} + \left(\frac{\sigma_0}{\rho} - \{\langle u_0\rangle\}\{\langle v_0\rangle\}\right) = U_1\{\langle v_0\rangle\} + U_\sigma^2, \tag{5.17}$$

where U_σ is the effective wall shear velocity, analogous to U_τ in the homogeneous case.
Now near the boundary $y = 0$ it is generally assumed that u' and v' are zero, and the region where this condition holds is termed the laminar sublayer. Actually, hot-wire measurements indicate that even in the sublayer time fluctuations are present but they are uncorrelated, i.e. $\langle u'v'\rangle = 0$, so that the shear stress is purely viscous and the mean flow behaves as though it were laminar. All the experimental evidence for the statement $\langle u'v'\rangle_0 = 0$ has however been obtained for $v_0 = 0$, and though the statement can reasonably be expected to be true if the boundary is uniformly porous

(with no discrete orifices and no space fluctuation), it may be false if discrete holes exist in the surface (and the flow is space-fluctuating as assumed in this section). Thus for homogeneous surfaces every quantity $q = \{q\}$ and $q^x \equiv 0$ and since $\langle u'v' \rangle_0 = 0$,

$$\sigma_0 = \mu \left(\frac{\partial \langle u \rangle}{\partial y} \right)_0 \equiv \tau_0 . \tag{5.18}$$

For non-homogeneous surfaces, however,

$$\sigma_0 = \mu \left(\frac{\partial \{\langle u \rangle\}}{\partial y} \right)_0 - \rho \langle \{u'\}\{v'\} \rangle_0 - \rho \{\langle u^x \rangle \langle v^x \rangle\}_0 - \rho \{\langle u'^x v'^x \rangle\}_0 , \tag{5.19}$$

and even if the Reynolds stress, $-\rho \langle u'v' \rangle$ should vanish, there remains the space-fluctuation stress, $-\rho\{\langle u^x \rangle \langle v^x \rangle\}$ which cannot be expected to vanish, so that the apparent wall shear cannot be identified with viscous shear (skin friction) as was the case for a homogeneous turbulent layer.

Provided the slip velocity $\{\langle u_0 \rangle\}$ is small (or even varying very slowly with x), the wall-region approximation

$$\{\langle u \rangle\} \frac{\partial \{\langle u \rangle\}}{\partial x} + \{\langle v \rangle\} \frac{\partial \{\langle u \rangle\}}{\partial y} = \{\langle v_0 \rangle\} \frac{\partial \{\langle u \rangle\}}{dy} \tag{5.20}$$

can be applied to a fluctuating as to a conventional layer. If the pressure-gradient term $(-1/\rho \, d\{\langle p \rangle\}/dx = U_1 \, dU_1/dx)$ is also neglected, equation (5.15) reduces to

$$\{\langle v_0 \rangle\} \frac{\partial \{\langle u \rangle\}}{\partial y} = \frac{1}{\rho} \frac{\partial \sigma}{\partial y} . \tag{5.21}$$

This can be integrated directly between 0 and y, giving

$$\frac{\sigma}{\rho} - \{\langle v_0 \rangle\}\{\langle u \rangle\} = \text{constant (w.r.t.y)} = \frac{\sigma_0}{\rho} - \{\langle v_0 \rangle\}\{\langle u_0 \rangle\} = U_\sigma^2 , \tag{5.22}$$

as in (5.17). If the fluctuations are confined within the wall region, then in the outer (homogeneous) portion of the wall region (5.22) still holds, whilst $\{\langle u \rangle\}$ now reduces to $\langle u \rangle$, σ to $\mu(\partial \langle u \rangle / \partial y) - \langle u'v' \rangle = \tau$, so that

$$\frac{\tau}{\rho} - \{\langle v_0 \rangle\}\langle u \rangle = U_\sigma^2 . \tag{5.23}$$

The mixing-length theory can be applied to this equation, yielding a bilogarithmic law for the velocity profile, just as in Section 2, with $\{\langle v_0 \rangle\}$ replacing v_0, and U_σ in the place of U_τ. κ can be expected to be the same for homogeneous and fluctuating layers, just as it is the same for smooth and rough surfaces, but the constant of integration must depend on the fluctuations just as A is a function of roughness when $v_0 = 0$.

It should be noted that although the quantity $\sigma_0/\rho - \{\langle u_0 \rangle\}\{\langle v_0 \rangle\}$ has been denoted by U_σ^2 as analogous to U_τ^2, there is no need for it to be greater than zero in the case of injection ($\{\langle v \rangle\} > 0$). For

$$U_\sigma^2 = \frac{\sigma_0}{\rho} - \{\langle v_0 \rangle\}\{\langle u_0 \rangle\} = \nu \left(\frac{\partial \{\langle u \rangle\}}{\partial y} \right)_0 - \{\langle u \rangle \langle v \rangle\}_0 ; \tag{5.24}$$

and at high rates of injection $\nu(\partial\{\langle u \rangle\}/\partial y)_0$ becomes very small, whilst $(uv)_0$ is essentially positive, so that its mean value may be larger than that of the viscous shear, yielding a negative apparent shear at the wall, $U_\sigma^2 < 0$.

6. *General Discussion of the Turbulent Boundary Layer with Transpiration.*

The purpose of this section is to present a physical picture of the turbulent boundary layer with transpiration, especially in the idealised case of a smooth homogeneous boundary. This picture is based mainly on a tentative interpretation of the meagre experimental data in existence.

6.1. *The Basic Mechanisms: Inner and Outer Regions.*

The turbulent boundary layer on a *solid* surface exhibits two distinct mechanisms. Thus in the region near the wall the flow is governed by the local conditions only and all the historical effects (the influence of the flow in the outer region) are confined to a single physical parameter which can be identified with the wall shear τ_0 or the wall shear velocity U_τ.

In the absence of a pressure gradient then, the velocity u depends only on y, ν and U_τ, and dimensional analysis indicates that u/U_τ must be a function of $U_\tau y/\nu$ only:

$$\frac{u}{U_\tau} = f\left(\frac{U_\tau y}{\nu}\right), \text{ 'law of the wall' (with } f \text{ a unique function).} \tag{6.1.1}$$

Pressure gradient introduces an additional variable, $(\nu/U_\tau^3)(1/\rho)dp/dx$, but it is found that a mild pressure gradient has negligible influence on the velocity distribution in the wall region (Fig. 14), so that equation (6.1.1) can be assumed to hold generally on a smooth solid surface.

The equation (6.1.1) is also modified when the flow in the immediate vicinity of the wall is not two-dimensional, e.g. due to roughness. In that case, if the effects of roughness can be described by a length scale k,

$$\frac{u}{U_\tau} = f\left(\frac{U_\tau y}{\nu}, \frac{U_\tau k}{\nu}\right), \tag{6.1.2}$$

or equally well

$$\frac{u}{U_\tau} = f_1\left(\frac{y}{k}, \frac{U_\tau k}{\nu}\right). \tag{6.1.3}$$

Transpiration introduces another physical quantity which must be included under the heading of 'local conditions', viz. the suction or injection velocity v_0, and so for smooth homogeneous walls and in zero pressure gradient the law of the wall must take the form

$$\frac{u}{U_\tau} = f\left(\frac{U_\tau y}{\nu}, \frac{v_0}{U_\tau}\right). \tag{6.1.4}$$

Obviously this can be rewritten as

$$\frac{u}{v_0} = f_2\left(\frac{v_0 y}{\nu}, \frac{v_0}{U_\tau}\right), \tag{6.1.5}$$

and in a variety of other ways.

The effects of a mild pressure gradient may again be expected to be negligible, whilst roughness or non-homogeneity of surface extend (6.1.4) to a form such as

$$\frac{u}{U_\tau} = f\left(\frac{U_\tau y}{\nu}, \frac{v_0}{U_\tau}, \frac{U_\tau k}{\nu}\right). \tag{6.1.6}$$

At large distances from the wall the flow does not respond immediately to a sudden change of conditions at the wall, and a wide variety of velocity distributions in the outer region could be

ed by suitable perturbations upstream. Various laws have however been found to hold in the gion of the solid boundary layer with fairly good accuracy. Ross[12] shows that Darcy's law for tre of a pipe

$$1 - \frac{u}{U_1} = D\left(1 - \frac{y}{\delta}\right)^{3/2}, \text{ with } D \text{ constant,} \tag{6.1.7}$$

es well the velocity profile near the edge of the layer. If the layer is allowed to settle in zero e gradient, Clauser[9] (Figs. 30, 31) demonstrates that the eddy viscosity $\epsilon\{= \tau/(\partial u/\partial y)\}$ is t across the outer region. It has also been found (*see* Coles[6]) that the plot of the velocity $U_1 - u$) against the wall distance, y, obeys a single-parameter law of the form

$$\frac{U_1 - u}{U_\tau} = g\left(\frac{y}{\delta}, \Pi(x)\right), \tag{6.1.8}$$

he parameter Π varies with x in general, but is constant in zero pressure gradient and in the ium layers of Clauser[16].

there exists a law determining the velocity distribution in the outer region, to which various mations have been found.

variation of velocity from the wall to the outer edge of the layer could, in general, take one of rms:

A sudden changeover from the wall law to that holding in the outer region (with a discontinuity of some derivatives of velocity),

An additional 'blending law' merging with those of the two basic regions, and

Overlap of the two laws.

(i) is physically unacceptable, whilst (ii) and (iii) can both arise, depending on the mation used in handling the problem. Thus overlap is impossible between the wall law nd the Darcy law (6.1.7) or the law obtained on the assumption of constant eddy viscosity is would relate terms involving dU_τ/dx with those supposedly dependent only on $U_\tau y/\nu$).) is far too general to produce useful results, as the 'blending law' would contain as many dent and dependent variables as the law for the boundary layer as a whole, so that the tion of the inner and outer laws would not reduce the complexity of the problem. It is e of great practical interest that, for the solid boundary, the law of the wall (6.1.2) is found to the velocity-defect law (6.1.8). By an argument similar to Millikan's[10] (cf. Section 3.2) it can n that if the ratio $(U_\tau y/\nu)/(y/\delta)$ can vary independently of $U_\tau k/\nu$ and $\Pi(x)$ (which is true ice), a logarithmic law for the velocity distribution in the overlap region is a condition of ncy. The observed logarithmic profile is therefore compatible with the velocity-defect law condition of overlap, but this does not imply that it is a consequence of the others. Indeed the mic law of the wall has been found by Klebanoff and Diehl[15] to hold even where the velocity- w does not, e.g. behind a tripping device.

the velocity-defect law in the form of (6.1.8) is a useful approximation in the solid case, t can be overlapped with the law of the wall, thus producing a complete description of the profile in the turbulent portion of the boundary layer. It cannot be a useful approximation some generalised form of equation (6.1.8) were found to hold] in a layer whose law of the not logarithmic, in particular it has been abandoned for the case of the layer with tion. Instead an alternative argument has been used by the authors to derive a law for the

velocity distribution (*see* Section 2). This is consistent with the logarithmic law of the wall and the velocity-defect law in the solid case, but is capable of describing accurately the profiles obtained with transpiration. It is based on the assumptions of momentum transfer theory with linear mixing length, summarised in the statement that, near a solid boundary {where $u(\partial u/\partial x) + v(\partial u/\partial y) \approx 0$},

$$\frac{\tau}{\rho} = \left(\kappa y \frac{\partial u}{\partial y}\right)^2. \tag{6.1.9}$$

This velocity/shear relationship is equally acceptable when the boundary is permeable and transpiration takes place. The logarithmic law holding on a solid surface can then be shown (Section 2) to be a particular case (with $v_0 = 0$) of the bilogarithmic law obtained on substituting (6.1.9) in the linearised equation of motion

$$\frac{1}{\rho}\frac{\partial \tau}{\partial y} = v_0 \frac{\partial u}{\partial y}, \tag{6.1.10}$$

i.e.

$$\frac{1}{\rho}(\tau - \tau_0) = v_0(u - u_0), \tag{6.1.11}$$

which holds in the vicinity of the boundary.

The bilogarithmic law has been demonstrated to hold both in the sucked and in the blown layers (Figs. 2 to 11), but it is realised that serious objections can be raised against the two basic premises, (6.1.9) and (6.1.10). Thus the argument of momentum transfer theory leading up to (6.1.9) associates the length scale κy (mixing length) with eddy diameter, but the large value of κ ($=0{\cdot}4$) observed in the (solid boundary) logarithmic law appears inconsistent with its physical meaning, as pointed out by Batchelor[18]. Furthermore the logarithmic law is found to hold well outside the region in which the quantities $u(\partial u/\partial x) + v(\partial u/\partial y)$ and $(\tau - \tau_0)$ are negligible, so that the combination of (6.1.9) and (6.1.11) (with $v_0 = 0$),

$$\left(\kappa y \frac{\partial u}{\partial y}\right)^2 = \frac{\tau_0}{\rho} = U_\tau^2, \tag{6.1.12}$$

holds even where neither of (6.1.9) and (6.1.11) does! It appears therefore that for solid boundaries (6.1.12) describes an empirical fact for which no completely satisfactory explanation is as yet available.

The equation (6.1.12) describes the relationship between the local velocity gradient and the overall drag experienced by the flow, with the wall distance y as a connecting link between the 'local' and the 'overall' quantities. The analogous form in the presence of transpiration can be deduced by considering the von Kármán momentum equation. Thus in a constant-pressure layer

$$\frac{d}{dx}(U_1^2\theta) = U_\tau^2 + v_0 U_1, \tag{6.1.13}$$

so that for the layer as a whole the quantity which is analogous to U_τ^2 in the solid case is $U_\tau^2 + v_0 U_1$. But near the wall the quantity U_1 has been found to have no effect [as in equation (6.1.6)], whilst at the wall itself U_τ^2 represents the true shear whether transpiration is applied or not. The analogue of U_τ^2 for the sucked (or blown) layer can therefore be expected to be the quantity $(U_\tau^2 + v_0 u)$, and so the basic equation for the transpiration layer becomes

$$\left(\kappa y \frac{\partial u}{\partial y}\right)^2 = U_\tau^2 + v_0 u = \frac{d}{dx}(U_1^2\theta) - v_0(U_1 - u). \tag{6.1.14}$$

This equation is identical with equation (2.2.16) and therefore leads directly to the bilogarithmic law (2.2.17).

The ultimate proof of equations (6.1.12) and (6.1.14) must await the solution of the full transient equations of turbulent flow, but this does not appear to be imminent. In the meantime they are justified by the good agreement between the velocity profiles observed in practice and those predicted by them.

The same criterion must be applied to the law describing the velocity distribution in the outer region: so far the most fruitful analysis of the outer region in a solid boundary layer has been that of Coles[6]. His wake law, whilst based on a tenuous analogy with free turbulent shear flow, describes actual boundary-layer velocity profiles with great accuracy and is therefore extended by the present authors to the case of transpiration (*see* Section 3).

Coles' wake hypothesis states in effect that in a layer which is not undergoing violent changes the velocity can be subdivided into two additive components. One of these is associated with the constraint imposed by the wall and obeys the law of the wall. The other, bound intimately with large scale mixing, is termed the 'wake component' by Coles in view of the similarity of its profile with that observed in a half-wake (also called the 'free-jet-boundary'—*see* Schlichting[19], p. 486).

$$u = u_c + u_w, \tag{6.1.15}$$

$$\frac{u_c}{U_\tau} = f\left(\frac{U_\tau y}{\nu}, \frac{U_\tau k}{\nu}\right) = A\left(\frac{U_\tau k}{\nu}\right) + \frac{1}{\kappa}\ln\frac{U_\tau y}{\nu}, \tag{6.1.16}$$

$$u_w = \frac{U_\tau}{\kappa}\,\Pi(x) w\left(\frac{y}{\delta}\right), \tag{6.1.17}$$

with $w(y/\delta)$ a unique function, of negligible magnitude near the wall (Coles' wake function) and $\Pi(x)$ a variable parameter (constant in zero pressure gradient).

It is clear that the mechanism producing the wake component cannot be destroyed by mild suction or injection at the wall, so that the velocity in a transpiration layer can again be expected to consist of two components, u_c obeying the law of the wall (6.1.4), and u_w taking the form

$$u_w = u_* \Pi(x) w(y/\delta). \tag{6.1.18}$$

Several forms of the wake law (6.1.18) are possible for the transpiration layer, depending on how the analogy of u_* with U_τ/κ is taken. The simplest form is obtained if u_* is taken to be constant (with respect to y) and equal to $(1/\kappa)U_\tau$,

$$u_w = \frac{U_\tau}{\kappa}\,\Pi(x) w\left(\frac{y}{\delta}\right). \tag{6.1.19}$$

An alternative form is obtained if u_* is identified with the quantity $y(\partial u_c/\partial y)$ which is equal to U_τ/κ when $v_0 = 0$ and appears to be of greater significance away from the wall than $\sqrt{(\tau_0/\rho)}$. Writing

$$y\frac{\partial u_c}{\partial y} = \frac{y U_\tau^2 \partial}{\nu \partial(U_\tau y/\nu)} f\left(\frac{U_\tau y}{\nu}, \frac{v_0}{U_\tau}\right) u_{*c}, \tag{6.1.20}$$

$$u_w = u_{*c} \Pi_*(x) w(y/\delta). \tag{6.1.21}$$

Other forms are obtained if different analogues of U_τ/κ are substituted for u_*, but it should be noted that those in which u_* is independent of y are experimentally indistinguishable from (6.1.19).

Thus if u_* is taken equal to $(1/\kappa)\sqrt{(U_\tau^2+v_0U_1)}$, which quantity appears to be more relevant outer region than U_τ/κ itself, the wake law can be written as

$$u_w = \frac{\sqrt{(U_\tau^2+v_0U_1)}}{\kappa}\,\Pi_1(x)w\left(\frac{y}{\delta}\right). \qquad (6.1.21)$$

The shape of the velocity profile is identical with that given by equation (6.1.19), only the v Π is affected.

Experimental evidence favours the choice of equation (6.1.21) rather than equations (6.1 (6.1.22).

To sum up briefly then, the turbulent portion of the transpiration layer consists of two regions—the wall region and the wake (outer) region, which show a marked similarity of be with the corresponding regions in a solid boundary layer.

6.2. *Types of Flow.*

The mutual influence of the outer and wall regions appears to be expressible as a single p quantity which can in general be identified with U_τ. The balance between the two tu régimes is therefore reflected in the relationship between U_τ and the other flow qua particularly U_1 and v_0. Three types of flow can then be distinguished:

(i) A conventional boundary layer is one in which the shear ρU_τ^2 is sufficiently large to ov the distorting effect of suction or injection on the turbulence in the layer so that the behaviou layer does not differ essentially from that in the case of solid boundaries. For this to be t following relationships must hold:

$$U_\tau^2 > 0,$$

$$U_\tau^2 + v_0U_1 > 0.$$

This class includes therefore all boundary layers on solid surfaces (except near separatio *undersucked* layers ($v_0 < 0$, $U_\tau^2 < -v_0U_1$) and presumably all layers with injection thr homogeneous surface (in which the wall shear cannot be negative though it might be zero). laws governing undersucked layers can be expected to have analogous forms applicable conventional layer with suction or injection. The bilogarithmic law (based on the linear v of mixing length) and Coles' wake hypothesis are two of the laws which have been applied report to boundary layers with $v_0 \neq 0$.

(ii) A *critical* boundary layer is one in which one or other of the inequalities (6.2.1), (6.2 ceases to be true. The constant pressure layer on a solid surface reaches this state asymptoti infinite downstream distance. Although it is impossible to obtain such a layer in practi tendencies observed in actual flows enable the properties of this layer to be determined. T rate of growth of the layer becomes zero (though its thickness is infinite), since the wall shear v Also the logarithmic law accounts for the entire velocity profile, since the maximum contr of the wake law to the value of u equation (3.3.5) is $2\Pi U_\tau/\kappa$, which vanishes when $U_\tau =$ Π remains finite in constant-pressure layers).

The layer with injection has been observed to reach the condition $U_\tau = 0$ at finite dista with finite thickness but it appears that this was due to the non-homogeneity of surface (cf., Se which is unavoidable in practice. Experimental evidence concerning the development of the layer with zero wall shear on a homogeneous surface is lacking and perhaps unobtainable, complete the argument it is surmised that in such a layer the streamwise velocity u w

negligible throughout the sublayer and part of the turbulent region so that the constraint velocity u_c would be effectively zero everywhere and the law of the wake would describe the entire layer which would behave like a free jet boundary.

In the case of injection equation (6.2.1) ceases to hold before equation (6.2.2) does, whilst for solid boundaries $v_0 = 0$ and the two equations are equivalent. When suction is applied, however, the critical condition is given by equation (6.2.2) which ceases to hold while U_τ^2 is still positive. It is seen from the momentum equation (2.2.9a) that the condition $U_\tau^2 + v_0 U_1 = 0$ implies (for constant-pressure layers) that the momentum thickness of the layer is constant, $d\theta/dx = 0$. It has in fact been found that such a layer quickly settles to the asymptotic state in which there is no variation of any of the flow quantities with x and that in fact the 'wake component' (i.e. departure from bilogarithmic velocity profiles) disappears completely. This state of affairs is consistent with the acceptance of $(U_\tau^2 + v_0 U_1)$ as the quantity describing the influence of the wall region on the outer portion of the layer and its use in conjunction with Coles' wake function as in equation (6.1.22) and also with the approach used to obtain equation (6.1.21). If equation (6.1.19) is accepted, then the value of Π_τ for asymptotic layers is zero.

(iii) The supercritical or *degenerate* form of the boundary layer does not occur in the presence of solid boundaries. With suction and injection, however, such a state is possible and is defined by

$$U_\tau^2 + v_0 U_1 < 0 \text{ for suction (oversucked)} \tag{6.2.3}$$

$$U_\tau^2 < 0 \text{ for injection (negative effective shear).} \tag{6.2.4}$$

The oversucked layer differs essentially from other turbulent layers in that its thickness is decreasing, whereas all others grow (this may not be true of layers in very strong favourable pressure gradients). The bilogarithmic law of the wall cannot hold throughout the oversucked layer, as the maximum velocity predicted by it $(= U_\tau^2/-v_0)$ is less than the free-stream velocity U_1, so that the strength of the wake component {defined as $(U_\tau/\kappa)\Pi_\tau w(1)$ in equation (6.1.19) or a corresponding expression in equations (6.1.21), (6.1.22)} must at least equal $(U_1 - U_\tau^2/-v_0)$. Experimental evidence does in fact suggest that the wake component of velocity in an oversucked layer has a profile different from that of Coles' wake function, whether plotted on the basis of u_w/U_τ or u_w/u_{*c}. This behaviour lends further weight to the argument in favour of calling an oversucked layer 'degenerate' and even though there are insufficient data for conclusive deductions to be made, an important change in the behaviour of the outer region as the layer becomes oversucked is to be expected, in view of the total disappearance of the wake component in the turbulent asymptotic layer.

The blown layer with negative effective wall shear could not be obtained on a homogeneous surface as it would necessarily have backflow near the surface. In spite of this, certain hypothetical predictions could be made regarding its behaviour. Such a layer would be growing with $d\theta/dx$ less than v_0/U_1, and the bilogarithmic law would not extrapolate to zero velocity at any value of wall distance y. It is clear that no statements can be made about the sublayer in such a case. A non-homogeneous boundary does make such a layer possible through the introduction of spatial-fluctuation shear (*see* Section 4) and layers showing this type of behaviour have in fact been obtained by Mickley and Davis[5]. The bilogarithmic and wake regions appear well behaved but the law of the wall cannot be extrapolated through the region of spatial fluctuations to the wall itself.

The picture which emerges from consideration of the three types of flow is that the effect of the outer region on the law of the wall is described entirely by the value of U_τ^2 and that when $U_\tau^2 = 0$,

$u = 0$ in the wall region, whilst for $U_\tau^2 < 0$ the flow near the wall departs from its normal behaviour. The effects of the wall conditions (constraint and transpiration) on the outer region are essentially described by the quantity $(U_\tau^2 + v_0 U_1)$, which vanishes simultaneously with the disappearance of the wake component in the asymptotic layer, whilst the outer region behaves abnormally when $U_\tau^2 + v_0 U_1 < 0$, (Fig. 14).

6.3. *Development of the Layer.*

Despite the scanty experimental evidence it is possible to predict qualitatively the development of a turbulent boundary layer with transpiration. Consider a layer with given initial conditions developing along a porous wall in zero pressure gradient and with constant v_0. After a short settling length in which the effects of discontinuity at the point where transpiration starts disappear, the behaviour of the layer will depend on the value of v_0/U_1.

At high injection rates the layer will grow rapidly, the rate of growth will decrease slowly to a constant value $d\theta/dx = v_0/U_1$ if the surface is homogeneous, and the layer will tend to assume a velocity profile like that at a free jet boundary. If the surface is non-homogeneous the rate of growth may decrease below that limiting value, yielding a layer with effective negative wall shear.

As the injection rate decreases so does the tendency of the layer to assume the form of the linearly growing half-jet, and the strength of the wake component decreases both with downstream distance for a given v_0 and with decreasing v_0 at a given station.

On a solid surface the thickness of the layer increases at a less than linear rate ($R_\theta \propto R_x^{4/5}$ approx.), the rate of growth tending to zero but reaching it only at infinite distance and thickness. The profile parameter Π is constant at a value of 0·55.

With a slight amount of suction the layer grows less rapidly and when some optimum rate of suction is applied the layer quickly reaches the asymptotic conditions of no streamwise variation and no wake component of velocity. Since the rate of growth tends to zero far downstream on a solid surface and quickly reaches zero at the optimum rate of suction, it is clear that the rate of growth will also tend to zero for growing sucked layers, but it has not yet been definitely established whether such layers grow indefinitely (at a decreasing rate) or their thickness tends to a finite value corresponding to the suction rate. Four distinct possibilities exist:

(i) For *every* suction rate $-v_0/U_1$ there is an asymptotic value of momentum-thickness Reynolds number $R_\theta = U_1\theta/\nu$ (or equivalently $-v_0\theta/\nu$) and conversely every value of asymptotic R_θ is obtainable by applying the corresponding suction.* When the asymptotic R_θ is very close to the value of R_θ at the beginning of suction the asymptotic conditions are reached very rapidly. If the two momentum thicknesses differ by much the asymptotic conditions are achieved at a large distance along the porous plate.

High suction rates correspond to thin asymptotic layers and *vice versa.*

(ii) There is a *unique* asymptotic suction rate which, when applied to a turbulent boundary layer, maintains it at its *initial* momentum thickness. At lower rates of suction the layer grows indefinitely whilst at higher suction rates it decreases in thickness and eventually reverts to the laminar state.

* At rates of suction higher than $(-v_0/U_1)_{\text{crit}}$ the turbulent layer will revert to laminar flow and reach the asymptotic conditions with $(-v_0\theta/\nu) = \frac{1}{2}$. There may be a discontinuity between this and the asymptotic turbulent value of $(-v_0\theta/\nu)$ for $(-v_0/U_1) \leqslant (-v_0/U_1)_{\text{crit}}$.

(iii) There is a *unique* asymptotic suction rate which, when applied to a layer, tends to increase or reduce it to a *unique* asymptotic thickness. The layer grows indefinitely with less suction and reverts to laminar flow with more.

(iv) There is a *unique* asymptotic suction rate which when applied to a layer of *unique initial* thickness, produces an asymptotic layer. In all other cases the layer either grows indefinitely or reverts to laminar flow.

The comparative ease with which asymptotic layers were obtained by Kay and by Dutton eliminates (iv). The assumption of the bilogarithmic law of the wall and the dependence of λ on v_0/U_τ makes (ii) also unacceptable, as, at the unique asymptotic suction rate, v_0/U_τ would be fixed and hence the corresponding value of $U_\tau d/\nu$, which in turn would yield a maximum value of $U_\tau\theta/\nu$* and so of $U_1\theta/\nu$ from which asymptotic conditions could be reached.

Dutton favours the third assumption but the coincidence that the unique asymptotic thickness was exactly the thickness of his boundary layer at the beginning of suction with his original entry conditions would be remarkable if it were correct, for whereas with the entry conditions altered Dutton found that the layer did not settle down to a constant state so readily, he did not attempt to obtain asymptotic conditions by adjusting the suction, i.e. he did not test the validity of (i) which appears the most acceptable to the present authors and has been neither confirmed nor disproved as yet.

At suction rates higher than the optimum (i.e. either the unique asymptotic or that producing an asymptotic layer of the same thickness as at entry) the layer at first decreases in thickness along the plate without reverting to laminar flow. If hypothesis (i) is true the reversion occurs when the suction rate exceeds a critical value, whilst according to (iii) it takes place when the Reynolds number R_θ has decreased sufficiently.

At very high suction rates the layer quickly reverts and reaches laminar asymptotic conditions with $(-v_0\theta/\nu) = \frac{1}{2}$†.

6.4. *Effects of Roughness and Non-Homogeneity of Surface.*

Discrete holes or pores through which suction or injection takes place cause the flow to be three-dimensional near the surface. These spatial fluctuations are smoothed out at large distances from the wall, so that the net effect of non-homogeneity is similar to that of roughness. Thus if the hole size and suction velocity are sufficiently small and the boundary layer sufficiently thick, the surface is aerodynamically smooth and homogeneous and the flow conforms to the idealised model.

As the size of the discrete orifices (or the suction velocity) increases, or as the layer becomes thinner, the spatial fluctuations cease to be negligible in an ever increasing proportion of the boundary layer. Outside the fluctuation region the flow mechanisms are unaffected: in particular the bilogarithmic constraint law and the wake law hold, but the inner boundary condition is changed, so that the values of the constant λ in the 'non-homogeneous' layer differ from those obtained in the ideal conditions with the same v_0 and effective wall shear expressed as U_σ (U_σ^2 is defined as $\tau_0/\rho - (u_0v_0)$, where the mean is taken with respect to space as well as time. In the ideal case $U_\sigma \equiv U_\tau$).

* $\left(\frac{U_\tau\theta}{\nu}\right)_{\max} = \frac{U_\tau}{\nu}\int_0^d \left[\left(\frac{v_0}{2\kappa}\ln\frac{y}{d}\right)^2 - U_\tau^2\right]\left[v_0U_1 - \left(\frac{v_0}{2\kappa}\ln\frac{y}{d}\right)^2 + U_\tau^2\right] \Big/ (v_0U_1)^2\,dy\,.$

† Dutton and Kay obtained asymptotic layers at the following suction rates: Dutton, smooth nylon surface $-v_0/U_1 = 0{\cdot}00443$; perforated surface: $-v_0/U_1 = 0{\cdot}0073$; Kay, sintered bronze $-v_0/U_1 = 0{\cdot}00332$. Dutton observed reversion at $-v_0/U_1 = 0{\cdot}0125$.

No attempt has been made as yet to obtain experimental results concerning the effective rou of a non-homogeneous surface, but the basic mathematical treatment of spatial fluctuati included in Section 5.

When the size of the fluctuations is comparable with the boundary-layer thickness the wl the wall region may be disturbed and no evidence exists regarding the flow in such a layer, l the whole it appears that the analogy between non-homogeneous transpiration and roughı fairly close, with one basic exception in that the boundary condition $u_0 = 0$ is not observe at the 'effective mean surface'. In particular the value of the quantity $\langle u_0 v_0 \rangle / U_1 \langle v_0 \rangle$ n appreciable, so that at high injection rates (for which τ_0 is small) the value of $\langle u_0 v_0 \rangle$ may be g than that of τ_0/ρ, resulting in negative effective wall shear U_σ^2, an impossible condition homogeneous surface, even with roughness.

As regards the development of the boundary-layer non-homogeneity tends to increase tl of growth of the layer with suction, so that a higher suction rate is required to maintain a at a given thickness.*

At zero transpiration only the roughness of the wall produces any fluctuations, so that l drilled sheet (surface Type D, Table 2.4.2), whilst behaving as a rough surface at high suctio developed a well-behaved smooth-plate layer in the absence of suction.

With blowing the effect of non-homogeneity is to make the layer grow more *slowly* than be the case on an ideal surface with the same injection rate and initial thickness, so that ef wall shear decreases below the limiting value of zero for the homogeneous wall.

In all cases then, the primary effect of non-homogeneity is to decrease the effectiven transpiration (provided $|v_0| \ll U_1$ everywhere).

The non-homogeneous surface may also be aerodynamically rough when no transpiratio place, but little distinction can be made between roughness and non-homogeneity effects $v_0 \neq 0$. It would, however, be of great interest to obtain experimental data concerning the fluct effects on surfaces of different geometry (hole size and spacing) and at different Reynolds nu (various v_0 and θ).

7. *Conclusions.*

The turbulent boundary layer with moderate suction or injection does not behave in an esse different manner from one developing on a solid wall. The laws holding on impervious surfac generally be extended by simple analogy to a form applicable to transpiration layers.

The most important of these is the bilogarithmic law of the wall in which the squared-logari term vanishes in the case of $v_0 = 0$. A method of plotting is available which determines th shear (and hence the growth of momentum thickness) from the local velocity distribution provided the local suction or injection velocity is known.

No reliable data are available on the velocity distribution within the sublayer, the lack of v however, is relatively unimportant as the effects of the sublayer on the velocity distribution fully turbulent region are confined to a single parameter (λ). The value of λ depends on th v_0/U_τ and, to a certain extent on the type of surface used.

The velocity distribution in the outer part of the transpiration layer conforms to the wak discovered by Coles and adapted to allow for the influence of suction or injection at the wall

* As shown by Dutton's asymptotic layers.

If sufficient suction is applied, the boundary layer can be maintained at constant thickness, or even thinned by the removal of more decelerated fluid than is entrained from the free stream. In the case of an oversucked layer, the Coles' wake law does not appear to describe the outer velocity profile with sufficient accuracy, but the law of the wall remains valid and the shear deduced from it agrees well with the von Kármán momentum equation.

Non-homogeneity of surface introduces spatial fluctuations near the wall. Their influence reduces the effectiveness of transpiration so that at the same transpiration rate, the effective wall shear (and so the growth of the layer) is higher for suction and lower for injection than through a homogeneous surface. In particular at high injection rates the effective wall shear can be negative.

There remains a great need for systematic data on the variation of the parameter λ, the correct reference velocity for the wake law and the effects of surface geometry and for the extension of both the theoretical analysis and the experiments to include the effects of pressure gradient.

The authors wish to express their gratitude to Dr. M. R. Head and Dr. B. G. Newman whose valued criticism helped our ideas to crystallise and for their unfailing support in the shaping of this paper. Our thanks also go to Professor W. A. Mair for many useful suggestions for the final presentation.

NOTATION

a, b		Constants in bilogarithmic law, equation (2.3.3)
a', b'		Constants in bilogarithmic law when $U_\tau^2 < 0$ equation (2.3.22)
A, B		Solid plate ($v_0 = 0$) values of a, b, equation (2.3.3a)
B_e, B_{10}		Values of B used in conjunction with ln and $\log_{10}$ equation (I.1)
d		Value of y at which u is a maximum (or a minimum) in the bilogarithmic law equation (2.3.1)
F, f, f_1, f_2, g		Denote functional dependence
i	$=$	$\sqrt{-1}$
L		Mixing length
m, n		Dimensionless transpiration rate and sublayer thickness, equations (4.3.1), (4.3.2)
N		Value of u/U_τ and $U_\tau y/\nu$ at transition point in the solid case equation (4.2.7)
n_s, n_i		Experimental parameters defined by equations (2.3.10), (2.3.14) for suction and injection respectively
p_s, p_i		Experimental parameters defined by equations (2.3.11), (2.3.15) for suction and injection respectively
p		Static pressure
q		An arbitrary constant used in Section 5
R_θ		Momentum thickness Reynolds number, $U_1\theta/\nu$
u, v, w		Velocities in x, y, z directions
U_1		Free-stream velocity
U_σ		Effective wall shear velocity for non-homogeneous surfaces, equation (5.17)
U_τ		Wall shear velocity for homogeneous surfaces, equation (2.2.7)
u_*		Local shear velocity, equation (6.1.18)
$w(y/\delta)$		Coles' wake function, equation (5.3.1)
w_τ, w_*		Experimental wake functions defined in Section 3.4
x, y, z		Space co-ordinates along, normal to, and across the plate
$x(t), y(t), z(t)$		Functions used and defined in Table 4.3.2 and Appendix III

y'	Effective wall distance discussed in Section 2.3.2
Y_s, Y_i	Co-ordinates used in plotting experimental results with suction and injection respectively, equations (2.3.8), (2.3.12)
δ	Boundary-layer thickness
δ^*	Boundary-layer displacement thickness
κ	Mixing-length coefficient defined by equation (2.1.1) and assumed to be a universal constant
λ	Profile parameter defined by equation (2.3.5)
λ'	Profile parameter defined by equation (2.3.23), used when $U_\tau^2 < 0$
μ, ν	Dynamic and kinematic viscosity ($\mu = \nu\rho$)
Π	Profile parameter defined by equation (3.3.1), used in conjunction with Coles' wake function
Π_τ, Π_*	Values of Π obtained under different suppositions (*see* Section 3.4)
ρ	Density of working fluid
σ, (σ_{ij})	Effective shear stress (and its full tensorial components) in space-fluctuating flow (*see* Section 5).
τ, (τ_{ij})	Shear stress in two-dimensional flow ($= \tau_{\text{visc}} + \tau_{\text{turb}}$)
τ_{visc}	Viscous shear stress ($= \mu \partial u/\partial y$)
τ_{turb}	Reynolds stress ($= -\rho\langle u'v' \rangle$)
θ	Momentum thickness
ϕ	Function used and defined in Table 4.3.2 and Appendix III

Subscripts

0	Conditions at the wall ($y = 0$)
a	Conditions at the transition point (edge of sublayer)
δ	Conditions at the edge of the boundary layer ($y = \delta$)
c	Quantities obtained from the bilogarithmic ('Constraint') law
w	Quantities obtained from the wake law
i, j	Running co-ordinates in tensorial analysis of Section 5

Superscripts

$'$	Denotes time fluctuations where applicable (*see* also a', b', λ', y')
x	Denotes spatial fluctuations
$\langle\ \rangle$	Denotes the time-mean
$\{\ \}$	Denotes the space-mean
$\|\ \|$	Placed round a quantity denotes the absolute value (modulus)
ln	Denotes $\log_e$
log	Denotes logarithm irrespective of base.

Special Terms

Solid	The word is used in its sense as an antonym to 'porous' to describe surfaces through which no transpiration takes place.
Spatial Fluctuation	The variation of a flow quantity about a mean in the x, z directions (due to discrete holes or roughness elements in the surface).
Non-homogeneous	Describes a surface and the boundary layer on it when spatial fluctuations are present.
Homogeneous	Surface and boundary layer with negligible spatial fluctuations.

REFERENCES

Author(s)	*Title, etc.*
M. Kay	Boundary-layer flow along a flat plate with uniform suction. A.R.C. R. & M. 2628. May, 1948.
A. Dutton	Experimental studies of the turbulent boundary layer. Ph.D. Thesis, Cambridge University. 1955. Published as The effects of distributed suction on the development of turbulent boundary layers. A.R.C. R. & M. 3155. March, 1958. See also A.R.C. C.P. 453. October, 1957.
H. Clarke, H. R. Menkes and P. A. Libby	A provisional analysis of turbulent boundary layers with injection. *J. Ae. Sci.*, Vol. 22, pp. 255 to 260. 1955.
W. Rubesin	An analytical estimation of the effect of transpiration cooling on the heat-transfer and skin-friction characteristics of a compressible turbulent boundary layer. N.A.C.A. Tech. Note 3341. December, 1954.
S. Mickley and R. S. Davis	Momentum transfer for flow over a flat plate with blowing. N.A.C.A. Tech. Note 4017. November, 1957.
Coles	The law of the wake in the turbulent boundary layer. *J. Fluid Mech.*, Vol. 1, pp. 191 to 226. 1956.
R. Van Driest	On turbulent flow near a wall. *J. Ae. Sci.*, Vol. 23, pp. 1007 to 1011 and p. 1036. 1956.
S. Mickley, R. C. Ross, A. L. Squyers and W. E. Stewart	Heat, mass, and momentum transfer for flow over a flat plate with blowing or suction. N.A.C.A. Tech. Note 3208. July, 1954.
H. Clauser	The turbulent boundary layer. *Adv. App. Mech.*, Vol. IV. 1956.
B. Millikan	A critical discussion of turbulent flows in channels and circular tubes. Proc. 5th Int. Cong. Appl. Mech., Cambridge, Massachusetts. pp. 386 to 392. 1938.
Liepmann and J. Laufer ..	Investigations of free turbulent mixing. N.A.C.A. Tech. Note 1257. August, 1947.
Ross	A study of incompressible turbulent boundary layers. Ph.D. Thesis, Harvard University. 1953.
Schultz-Grunow	New frictional resistance law for smooth plates. (English translation.) N.A.C.A. Tech. Memo. 986. September, 1941.
Ludwieg and W. Tillmann..	Investigations of the wall-shearing stress in turbulent boundary layers. (English translation.) N.A.C.A. Tech. Memo. 1285. May, 1950.

REFERENCES—*continued*

No.	*Author(s)*	*Title, etc.*
15	P. S. Klebanoff and Z. W. Diehl	Some features of artificially thickened fully developed turbulent boundary layers with zero pressure gradient. N.A.C.A. Report 1110. 1952.
16	F. H. Clauser	Turbulent boundary layers in adverse pressure gradients. *J. Ae. Sci.*, Vol. 21, pp. 91 to 108. 1954.
17	D. Coles	The law of the wall in turbulent shear flow. *50 Jahre Grenzschichtforschung*, pp. 153 to 163, Friedr. Vieweg & Sohn, Braunschweig. 1955.
18	G. K. Batchelor	Note on free turbulent flows, with special reference to the two-dimensional wake. *J. Ae. Sci.*, Vol. 17, pp. 441 to 445. 1950.
19	H. Schlichting	*Boundary layer theory*. (English translation.) Pergamon Press Ltd., London. 1955.

APPENDIX I

Values of the Constants in the Logarithmic Law with Zero Transpiration

The velocity distribution in the turbulent wall region of a boundary layer on a solid wall is known to be described by the logarithmic law

$$\frac{u}{U_\tau} = A + B_{10} \log_{10} \frac{U_\tau y}{\nu} = A + B_e \ln \frac{U_\tau y}{\nu}. \tag{I.1}$$

The coefficients A and B are accepted by all investigators as being constant for all layers on smooth flat surfaces, but there is a considerable amount of disagreement regarding their actual values, as can be seen from Table I.1 (cf. Table 3.1, Ross[12]).

TABLE I.1

Constants A and B in the Flat-Plate Logarithmic Law

Investigator	A	B_{10}	Method of determining wall shear	Max value of $U_\tau y/\nu$	$A+2B_{10}$
Schultz-Grunow[13]	4·07	5·93	Floating element	500	15·9
Ludwieg and Tillmann[14]	6·0	5·2	Heat transfer	500	16·4
Klebanoff and Diehl[15]	4·8	5·4	Momentum integral equation	500	15·6
Clauser[16]	4·9	5·6			16·1
Coles[17]	5·1	5·75	Floating element		16·6
Dutton[2]*	5·8	5·5	Preston tube	200	16·8
	6·1	5·4			16·9
Sarnecki (unpublished)†	5·5	5·1	Momentum integral equation	250	16·7

* Dutton used Nikuradse's values (4·8, 4·5) as a basis for comparison of his experimental profiles with theory. The agreement was good, but his experimental points lie consistently above the line and a better fit is obtained by using (5·1, 4·4).

† Unpublished results obtained in conditions similar to those of the suction experiments shown in Figs. 2, 3, but with the perforated surface covered with (impervious) tracing linen. Spanwise variation of velocity in the boundary layer at a given height from the surface did not exceed 1% of U_1. Scatter of experimental points about the line $A = 5{\cdot}5$, $B = 5{\cdot}1$ not more than 1% of U_1. Values of R_θ between 1000 and 3500.

The above values of A and B predict velocities in the boundary layer differing by as much as 10% of u and two alternatives appear. Either A and B are not universal constants for smooth flat plates, or the discrepancies are due to different interpretations of experimental data. If the former is to be discounted, a way must be sought to adjust the results of the various investigators, so that they all conform to a universal law.

There are two sources of error in the experimental determination of A and B. One is the problem of finding the true value of skin friction and so the correct scale of u/U_τ and $U_\tau y/\nu$. Five distinct methods have been used by various investigators for the flat-plate layer. These are:

(i) the momentum integral equation (differentiation of the experimental values of θ)

(ii) the floating element (direct measurement of force on a movable plate)

(iii) the Preston tube (round pitot tube on the surface of the plate; calibrated in a pipe)

(iv) the Stanton tube

(v) heat transfer (direct relationship between skin-friction and heat loss).

These methods do not give very good agreement with one another and none appears to be basically more sound that the others, although (i) is perhaps the least reliable.

Now the flat-plate log-law can be written

$$\frac{u}{BU_\tau} = \left(\frac{A}{B} - \log B\right) + \log \frac{BU_\tau y}{\nu} \tag{I.2}$$

so that in any experiment $(A/B - \log B)$ and (BU_τ) are obtainable directly from the velocity distribution, and any adjustment of U_τ will be reflected in an adjustment of A and B, with $(A/B - \log B)$ invariant; thus two different sets of A and B may be consistent, subject to the adjustment of U_τ, provided $A/B - \log B$ is the same in both cases.

A second source of error lies in the choice of the 'best' straight line through a set of experimental points. It has in fact been observed that the graph of u against $\log y$ is not perfectly straight, but slightly concave upwards (near the edge of the sublayer some points appear to lie above the line of the log-law, (cf. Coles[10] Figs. 1 to 17) so that different values of slope (over a small range) can be obtained from the same set of points, though each reasonable curve *must* pass close to the experimental points near $U_\tau y/\nu = 100$. For comparison therefore, the values of A and B have been adjusted for each of the eight formulae of Table I.1, keeping $(A/B - \log B)$ constant in each case, so as to give lines intersecting at $U_\tau y/\nu = 100$, $u/U_\tau = 16{\cdot}4$. (The value 16·4 is the average of the eight values of $A + 2B$ in Table I.1) Table I.2 shows these adjusted values of A and B (together with other possible values satisfying $A + 2B = 16{\cdot}4$).

TABLE I.2

Adjustment of U_τ to Give Lines Intersecting at $U_\tau y/\nu = 100$

Investigator	Original		$A/B - \log B$	A	B	Necessary adjustment in U_τ
	A	B				
—	—	—	0·581	6·4	5·0	—
—	—	—	0·508	6·2	5·1	—
Ludwieg and Tillmann	6·0	5·2	0·438	6·0	5·2	Nil
Dutton	6·1	5·4	0·398	5·88	5·26	+2·7%
Sarnecki	5·5	5·1	0·370	5·8	5·3	−3·8%
Dutton (Nikuradse)	5·8	5·5	0·313	5·64	5·38	+2·2%
—	—	—	0·304	5·6	5·4	—
—	—	—	0·242	5·4	5·5	—
—	—	—	0·181	5·2	5·6	—
Klebanoff and Diehl	4·8	5·4	0·147	5·12	5·64	−4·3%
Clauser	4·9	5·6	0·127	5·02	5·69	−1·6%
Coles	5·1	5·75	0·126	5·01	5·69	+1·1%
—	—	—	0·122	5·0	5·7	—
—	—	—	0·064	4·8	5·8	—
—	—	—	+0·009	4·6	5·9	—
—	—	—	−0·044	4·4	6·0	—
Schultz-Grunow	4·07	5·93	−0·086	4·24	6·08	−2·5%

Table I.3 shows the degree of adjustment necessary for U_τ obtained by different methods.

TABLE I.3

Adjustment to U_τ obtained by Different Methods

Method	Investigator	Adjustment
Preston tube	Dutton	+2·7%
		+2·2%
Heat transfer	Ludwieg and Tillmann	Nil
Floating element	Coles	+1·1%
	Schultz-Grunow	−2·5%
(Not stated)	Clauser	−1·1%
Momentum integral equation	Sarnecki	−3·8%
	Klebanoff and Diehl	−4·3%

Fig. 19 shows the graphs of u/U_τ against $U_\tau y/\nu$ obtained with the extreme values of A and B from Table I.2 (i.e. Ludwieg and Tillmann's and Schultz-Grunow's). It is seen that the disparity is not great and that a line with $B = 5{\cdot}5$ provides a good mean with departures from it not greater than 2% of u. The value $B = 5{\cdot}5$ and the corresponding $A = 5{\cdot}4$ have therefore been accepted for the analysis of experimental results.

APPENDIX II

Note on the Use of Logarithms in Calculations Involving the Bilogarithmic Law

The functions $\log_{10} q$ and $\ln q$ both appear in the present paper, as ln is the natural choice for theoretical work and $\log_{10}$ is more convenient in calculations. No confusion need arise provided it is realised that the coefficient B has different values when multiplying a natural or a decimal logarithm. The two values are denoted by B_e and B_{10} where necessary. Thus $1/\kappa = B_e$ whereas B_{10} is the slope of the straight line in Fig. 19.

TABLE II.1

Accepted Values of Constants appearing in Calculations

Constant	Value	Logarithm ($\log_{10}$)
A	5·4	0·732394
B_{10}	5·5	0·740363
B_e	2·39	0·378147
κ	0·419	$\bar{1}$·621853
N	11·2	1·047771
$1/N$	0·0896	$\bar{1}$·952229
$2/N$	0·179	$\bar{1}$·253259
B_{10}/N	0·493	$\bar{1}$·692592
B_e/N	0·214	$\bar{1}$·330376
A/N	0·484	$\bar{1}$·684623
$1 - A/N$	0·516	$\bar{1}$·712858

Note. N is the value of u/U_τ and $U_\tau y/\nu$ at the intersection of the linear (sublayer) and logarithmic (turbulent) wall laws, equations (4.1.2) and (2.3.3a).

APPENDIX III

Detailed Analysis of Possible Criteria for Transition from Sublayer to Fully Turbulent Wall Law

Table 4.3.1 lists the 13 simplest parameters and their values at the transition point (i.e. edge of the sublayer) in the case of solid boundaries. Each of these {except (vii), (viii) and (x) which do not vary in the solid case} is acceptable as a possible transition criterion in the general case of transpiration. The assumption of any one of them yields a relationship between the sublayer thickness y_a and the transpiration and shear velocities v_0 and U_τ, or in dimensionless terms between $m\ [= (N/2)(v_0/U_\tau)]$ and $n\ [= (1/N)(U_\tau y_a/\nu)]$. Since λ is given in terms of m and n by equation (4.3.9) each criterion leads to an expression for λ in terms of m (i.e. of v_0/U_τ) only, as follows:

(i) $$\frac{U_\tau y_a}{\nu} = N, \text{ i.e. } Nn = N, \tag{III.1}$$

$$n = 1,$$

$$\lambda = e^m - m\frac{B}{N}\log N. \tag{III.2}$$

(ii) $$\frac{u_a}{U_\tau} = N, \text{ i.e. } \frac{N}{2m}(e^{2mn}-1) = N,\ e^{2mn} = 1+2m,$$

$$n = \frac{1}{2m}\ln(1+2m). \tag{III.3}$$

$$\lambda = \sqrt{(1+2m)} - m\frac{B}{N}\log\left[\frac{\ln(1+2m)}{2m}\right] - m\frac{B}{N}\log N. \tag{III.4}$$

This gives a real result only if $\dfrac{\ln(1+2m)}{2m} > 0$, i.e. if

$$m > -\tfrac{1}{2}. \tag{III.5}$$

Unless $m > -\frac{1}{2}$ the value of $u = NU_\tau$ is never attained by the sublayer law.

(iii) $$\frac{u_a y_a}{\nu} = N^2, \text{ i.e. } U_\tau\frac{N}{2m}(e^{2mn}-1)\frac{Nn}{U_\tau} = N^2,$$

$$\frac{n}{2m}(e^{2mn}-1) = 1,$$

$$mne^{mn}\sinh(mn) = m^2,$$

hence

$$n = \frac{1}{m}x(m), \tag{III.6}$$

where $x(t)$ is defined by

$$xe^x\sinh x = t^2. \tag{III.7}$$

$$\lambda = e^{x(m)} - m\frac{B}{N}\log\frac{x(m)}{m} - m\frac{B}{N}\log N. \tag{III.8}$$

(iv) $\dfrac{y_a^2}{\nu}\left(\dfrac{\partial u}{\partial y}\right)_a = N^2$ in the sublayer law, i.e. $\dfrac{\nu}{U_\tau^2}(Nn)^2\dfrac{U_\tau^2}{\nu}e^{2mn} = N^2$,

$$(ne^{mn})^2 = 1,\ ne^{mn} = 1,$$

$$mne^{mn} = m,$$

hence

$$n = \frac{1}{m}y(m), \tag{III.9}$$

where $y(t)$ is defined by

$$ye^y = t, \tag{III.10}$$

and, for real y, $t \geqslant -\dfrac{1}{e}$.

$$\lambda = e^{y(m)} + \frac{m}{\kappa N}y(m) - m\frac{B}{N}\log N, \tag{III.11}$$

provided that

$$m > -\frac{1}{e} = -0{\cdot}368. \tag{III.12}$$

For greater negative values of m the value of $(y^2/\nu)\partial u/\partial y$ in the sublayer law is always less than N^2.

(v) $\dfrac{y_a^2}{\nu}\left(\dfrac{\partial u}{\partial y}\right)_a = \dfrac{N}{\kappa}$ in the turbulent law, i.e. $\dfrac{\nu}{U_\tau^2}(Nn)^2\dfrac{U_\tau^2}{\nu}\dfrac{1}{\kappa Nn}e^{mn} = \dfrac{N}{\kappa}$,

$ne^{mn} = 1$, result identical with (iv).

(vi) $\dfrac{y_a}{U_\tau}\left(\dfrac{\partial u}{\partial y}\right)_a = N$ in the sublayer law, i.e. $\dfrac{\nu}{U_\tau^2}Nn\dfrac{U_\tau^2}{\nu}e^{2mn} = N$,

$$ne^{2mn} = 1,\ 2mne^{2mn} = 2m,$$

$$n = \frac{1}{2m}y(2m), \tag{III.13}$$

with $y(t)$ defined by (III.10).

$$\lambda = e^{1/2y(2m)} + \frac{m}{\kappa N}y(2m) - m\frac{B}{N}\log N \tag{III.14}$$

provided

$$2m > -\frac{1}{e},\ m > -0{\cdot}184. \tag{III.15}$$

(ix) $\dfrac{u_a}{y_a\left(\dfrac{\partial u}{\partial y}\right)_a} = \kappa N$ in the turbulent law, i.e. $\dfrac{U_\tau\dfrac{N}{2m}(e^{2mn}-1)}{\dfrac{\nu}{U_\tau}Nn\dfrac{U_\tau^2}{\nu}\dfrac{1}{\kappa Nn}e^{mn}} = \kappa N$,

$$\frac{1}{2m}\frac{e^{2mn}-1}{e^{mn}} = 1,\ \sinh mn = m.$$

Putting

$$m = \sinh \phi, \tag{III.16}$$

$$n = \frac{\phi}{m} = \frac{\phi}{\sinh \phi}. \tag{III.17}$$

$$\lambda = e^{\phi} + m \frac{B}{N} \log \frac{\sinh \phi}{\phi} - m \frac{B}{N} \log N. \tag{III.18}$$

(xi) $$\frac{U_\tau^2}{\nu \left(\frac{\partial u}{\partial y}\right)_a} = \kappa N \text{ in the turbulent law, i.e. } \frac{\kappa N n}{e^{mn}} = \kappa N,$$

$$ne^{-mn} = 1, \quad -mne^{-mn} = -m,$$

$$n = -\frac{1}{m} y(-m), \tag{III.19}$$

defining $y(t)$ as in (III.10).

$$\lambda = e^{-y(-m)} + \frac{m}{\kappa N} y(-m) - m \frac{B}{N} \log N, \tag{III.20}$$

provided $m < \frac{1}{e} = 0{\cdot}368$, a critical *injection* rate (III.21)

(xii) $$\frac{u_a^2}{\nu \left(\frac{\partial u}{\partial y}\right)_a} = N^2 \text{ in the sublayer law, i.e. } \frac{U_\tau^2 \frac{N^2}{(2m)^2} (e^{2mn} - 1)^2}{U_\tau^2 e^{2mn}} = N^2,$$

$$\frac{1}{2m} \frac{e^{2mn} - 1}{e^{mn}} = 1, \text{ as in (ix)}.$$

(xiii) $$\frac{u_a^2}{\nu \left(\frac{\partial u}{\partial y}\right)_a} = \kappa N^3 \text{ in the turbulent law, i.e. } \frac{U_\tau^2 \frac{N^2}{(2m)^2} (e^{2mn} - 1)^2}{U_\tau^2 \frac{1}{\kappa N n} e^{mn}} = \kappa N^3,$$

$$\frac{n}{m^2} e^{mn} \sinh^2 (mn) = 1, \quad mne^{mn} \sinh^2 (mn) = m^3,$$

$$n = \frac{1}{m} z(m), \tag{III.22}$$

where $z(t)$ is given by

$$ze^z \sinh^2 z = t^3. \tag{III.23}$$

$$\lambda = e^{z(m)} - m \frac{B}{N} \log \frac{z(m)}{m} - m \frac{B}{N} \log N. \tag{III.24}$$

Note that the term $-m(B/N) \log N$ which occurs in all the expressions for λ can also be written as $m(A/N - 1)$, since $B \log N = N - A$. The values of λ for different v_0/U_τ have been computed from each of the equations (III.2), (III.4), (III.11), (III.18), (III.20) and (III.24). They are tabulated in Table III.1 and plotted in Fig. 13a.

TABLE III.1

Computed Values of λ for different Transition Criteria

Criterion (i)

v_0/U_τ	λ
−0·179	0·884
−0·143	0·862
−0·107	0·859
−0·072	0·878
−0·036	0·922
0	1·000
+0·036	1·118
0·072	1·285
0·107	1·512
0·143	1·813
0·179	2·202
0·215	2·701
0·251	3·332
0·287	4·127
0·323	5·110
0·358	6·358
0·394	7·889
0·430	9·784
0·466	12·121
0·502	14·999
0·538	18·537

Criterion (ii)

v_0/U_τ	λ
−0·0896	+ ∞
−0·0895	0·496
−0·0890	0·508
−0·0878	0·540
−0·0860	0·572
−0·0842	0·598
−0·0824	0·620
−0·0806	0·639
−0·0717	0·714
−0·0627	0·769
−0·0538	0·815
−0·0448	0·854
−0·0358	0·888
−0·0269	0·920
−0·0179	0·948
−0·0090	0·975
0	1·000
+0·018	1·046
0·036	1·087
0·054	1·126
0·072	1·162
0·090	1·195
0·107	1·227
0·125	1·258
0·143	1·288
0·161	1·316
0·179	1·344
0·215	1·397
0·251	1·448
0·287	1·498
0·323	1·546
0·358	1·593
0·394	1·640
0·430	1·685
0·466	1·730
0·502	1·775
0·538	1·820
0·896	2·263
1·792	3·448

TABLE III.1—*continued*

Criterion (iii)

v_0/U_τ	λ
−0·118	0·766
−0·101	0·783
−0·082	0·812
−0·059	0·855
−0·033	0·916
0	1·000
+0·040	1·112
0·089	1·259
0·149	1·450
0·225	1·698
0·320	2·018
0·439	2·429
0·661	2·916
0·777	3·639
1·014	4·515
1·312	5·642
1·685	7·093
2·155	8·962
2·743	11·355
3·480	14·467
4·402	18·457

Criterion (iv) or (v)

v_0/U_τ	λ
−0·0001	0·001
−0·0060	0·060
−0·0485	0·391
−0·0579	0·479
−0·0619	0·528
−0·0648	0·581
−0·0656	0·608
−0·0659	0·637
−0·0656	0·666
−0·0644	0·696
−0·0590	0·761
−0·0480	0·832
−0·0293	0·910
0	1·000
+0·044	1·106
0·107	1·216
0·196	1·398
0·319	1·610
0·487	1·897
0·714	2·287
1·017	2·825
1·420	3·575
1·951	4·622
2·648	7·085
3·557	8·122
4·731	10·340
6·272	14·938

TABLE III.1—*continued*

Criterion (vi)

v_0/U_τ	λ
−0·0000	0·000
−0·0000	0·007
−0·0066	0·186
−0·0117	0·280
−0·0195	0·413
−0·0242	0·496
−0·0289	0·588
−0·0324	0·689
−0·0322	0·794
−0·0240	0·899
0	1·000
+0·053	1·093
0·159	1·185
0·357	1·305
0·710	1·537
1·324	2·081
2·370	3·316
4·125	5·964
7·033	11·567
11·803	20·79

Criterion (ix) or (xii)

v_0/U_τ	λ
−0·211	0·934
−0·159	0·888
−0·114	0·869
−0·074	0·880
−0·036	0·922
0	1·0
+0·036	1·118
0·074	1·282
0·114	1·502
0·159	1·787
0·211	2·152
0·270	2·615
0·341	3·197
0·426	3·928
0·527	4·840
0·650	5·979
0·799	7·397
0·979	9·164
1·199	11·363
1·468	14·097
1·795	17·498

Criterion (xi)

v_0/U_τ	λ
−0·487	1·190
−0·319	1·064
−0·196	0·973
−0·107	0·946
−0·044	0·934
0	1·000
+0·0293	1·130
0·0480	1·330
0·0590	1·610
0·0644	1·978
0·0656	2·200
0·0659	2·450
0·0656	2·729
0·0648	3·041
0·0619	3·774
0·0579	4·676
0·0485	7·133
0·0060	148·4
0·000081	22027

Criterion (xiii)

v_0/U_τ	λ
−0·143	0·818
−0·118	0·816
−0·092	0·830
−0·064	0·863
−0·034	0·918
0	1·000
+0·038	1·114
0·083	1·267
0·137	1·468
0·201	1·728
0·278	2·063
0·374	2·490
0·491	3·033
0·636	3·726
0·815	4·606
1·038	5·717
1·314	7·128
1·657	8·918
2·082	11·203
2·610	14·065
3·264	17·713

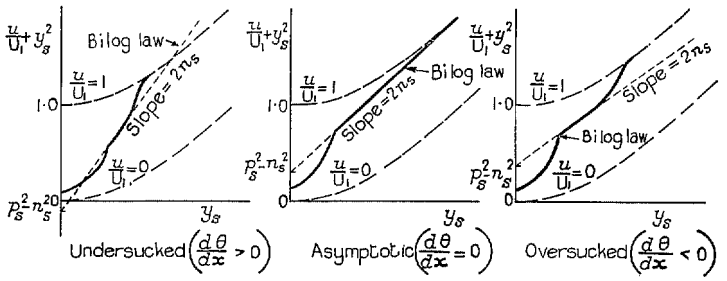

FIG. 1a. Typical suction profiles.

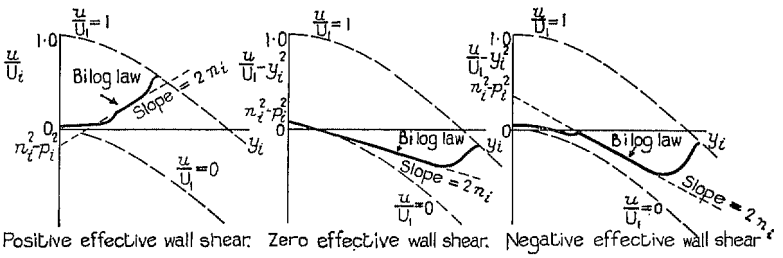

FIG. 1b. Typical injection profiles.

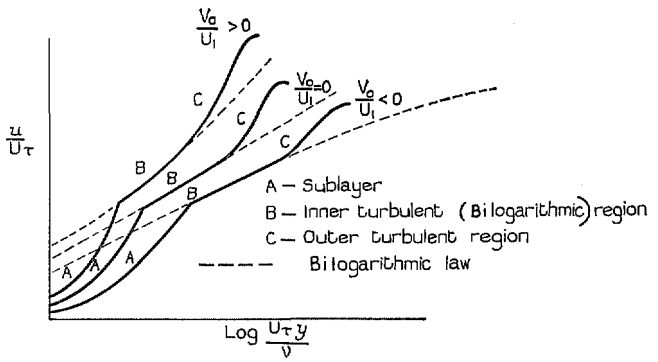

FIG. 1c. Orthodox plot of typical velocity profiles.

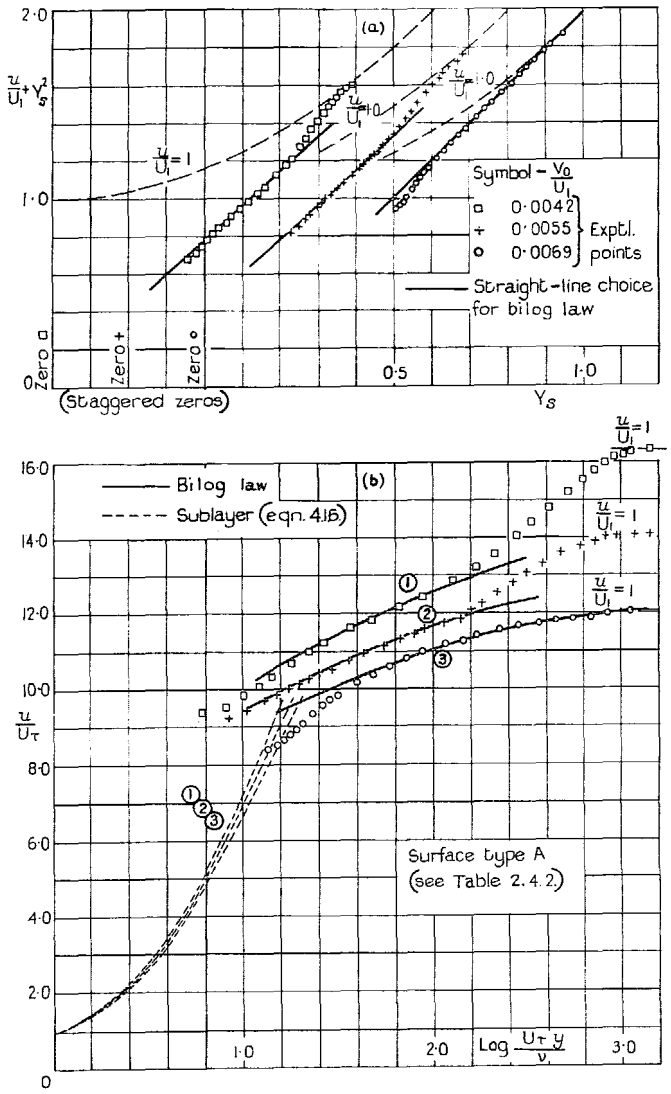

FIG. 2. Velocity profiles obtained by Sarnecki with suction through a perforated surface.

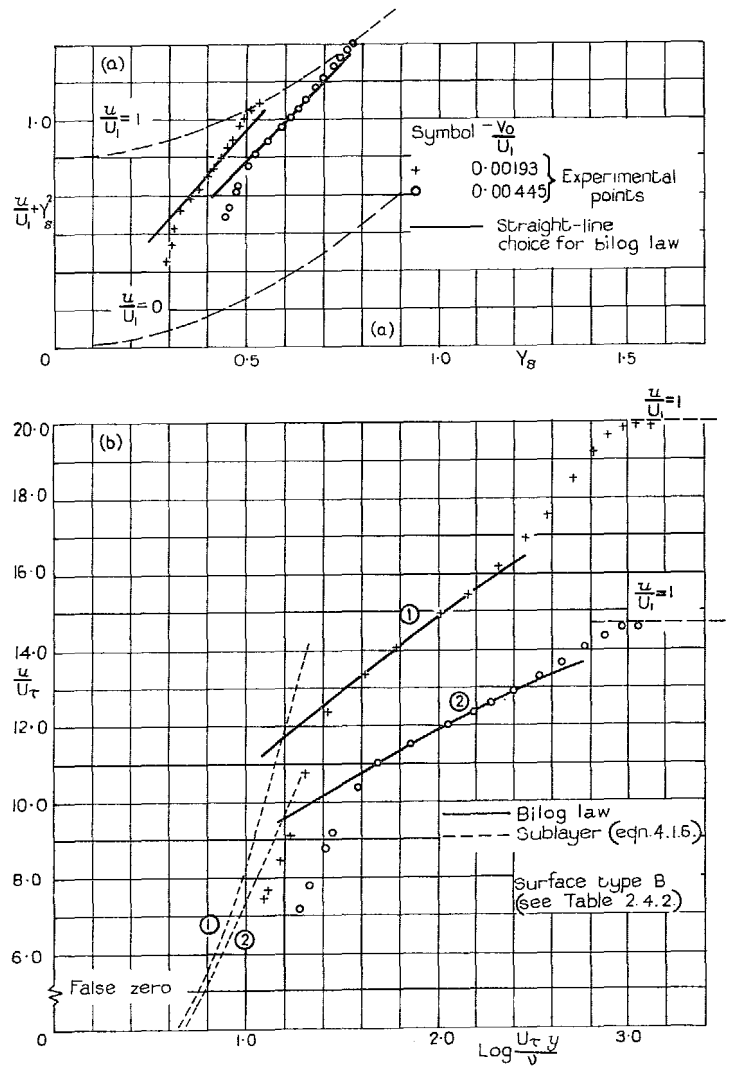

FIG. 3. Velocity profiles obtained by Sarnecki with suction through a nylon surface.

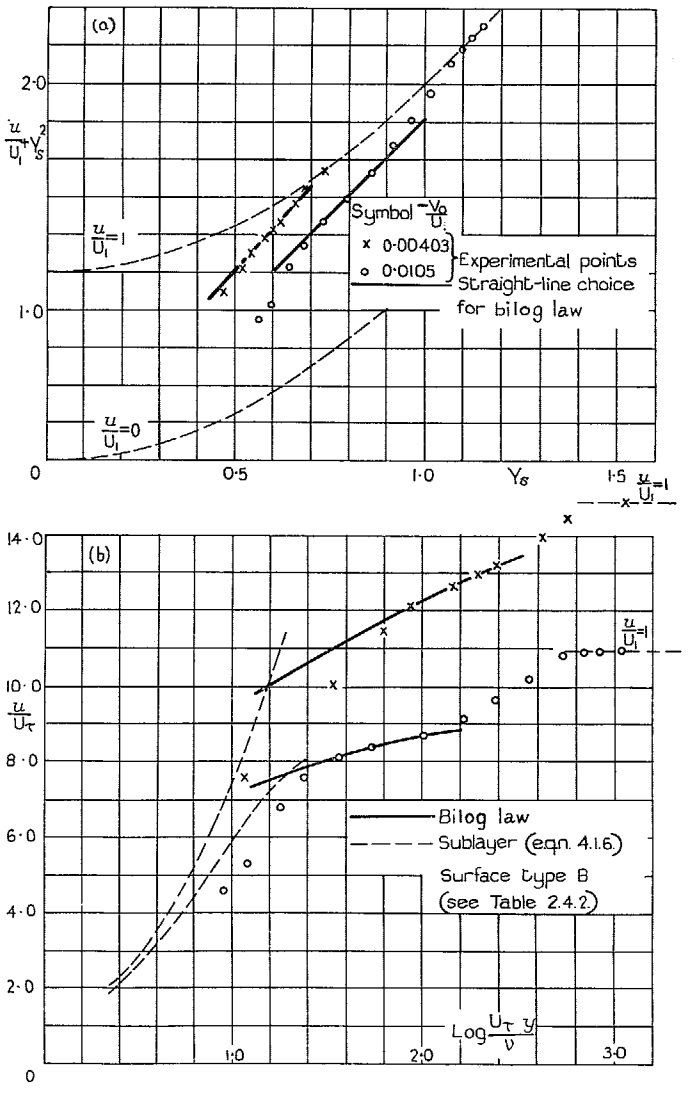

FIG. 4. Velocity profiles obtained by Dutton with suction through a nylon surface.

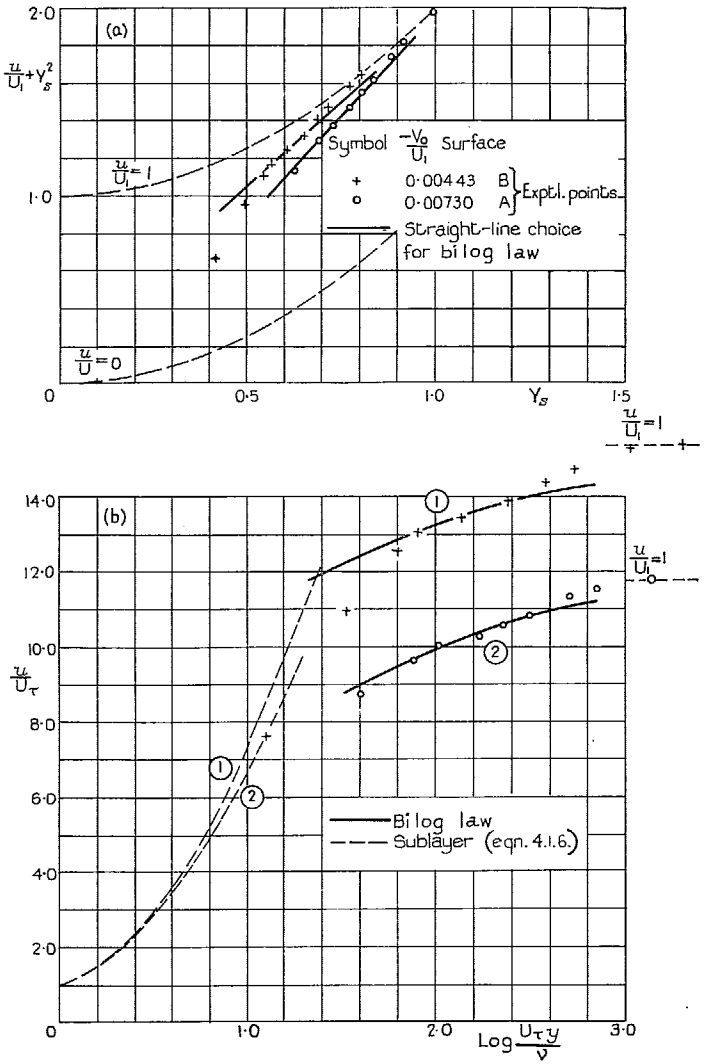

FIG. 5. Velocity profiles in Dutton's asymptotic layers.

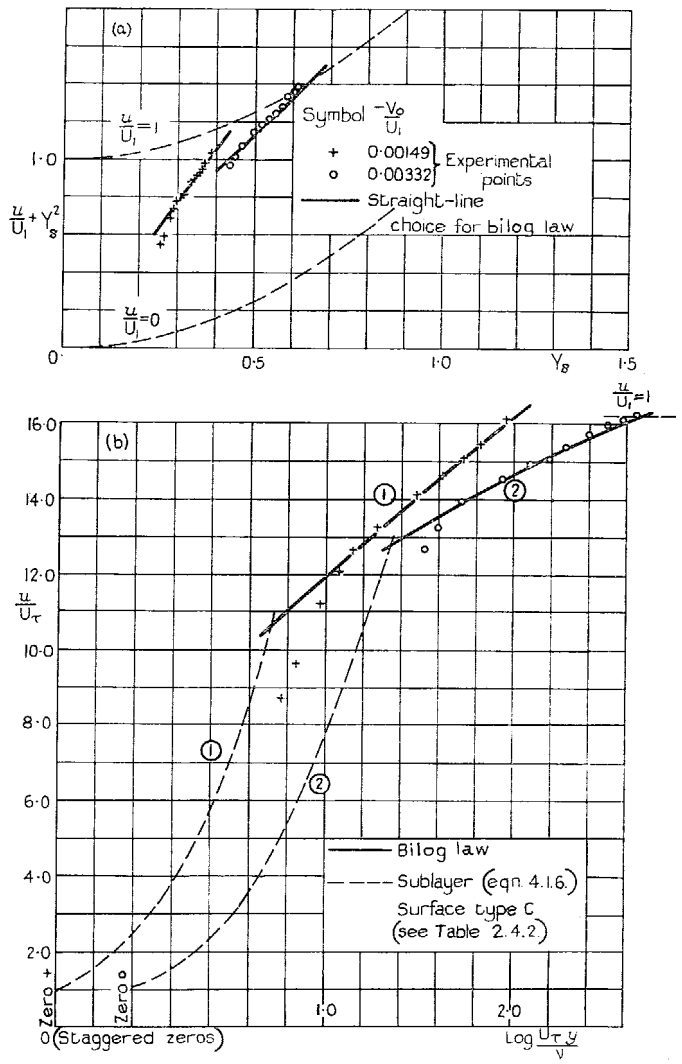

FIG. 6. Velocity profiles obtained by Kay with suction through a porous surface.

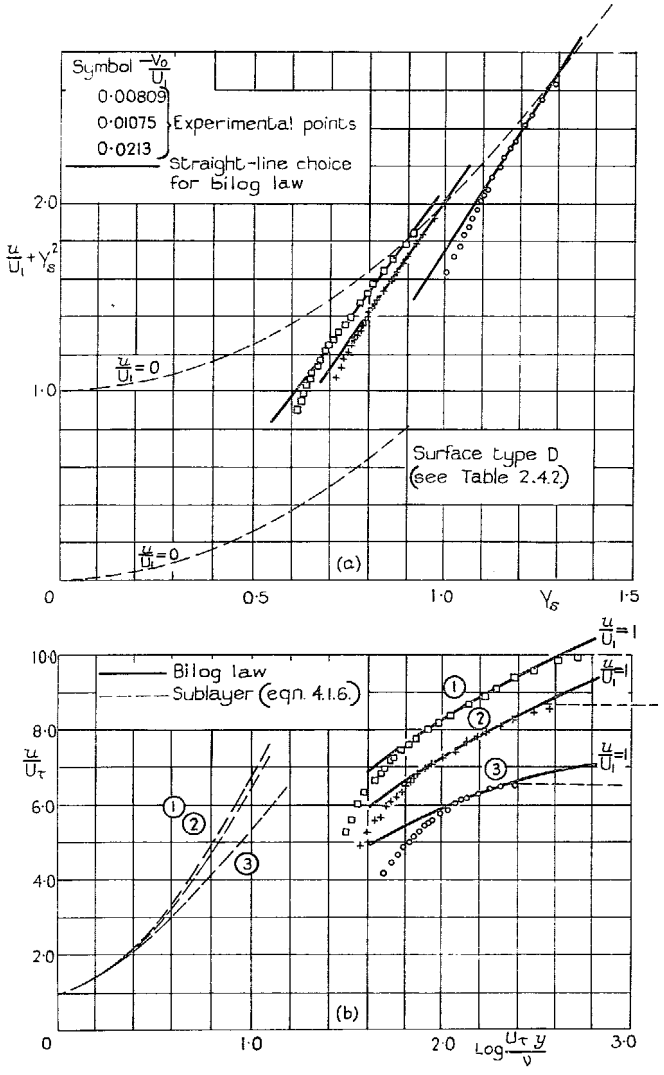

FIG. 7. Velocity profiles obtained by Black with suction through a drilled surface.

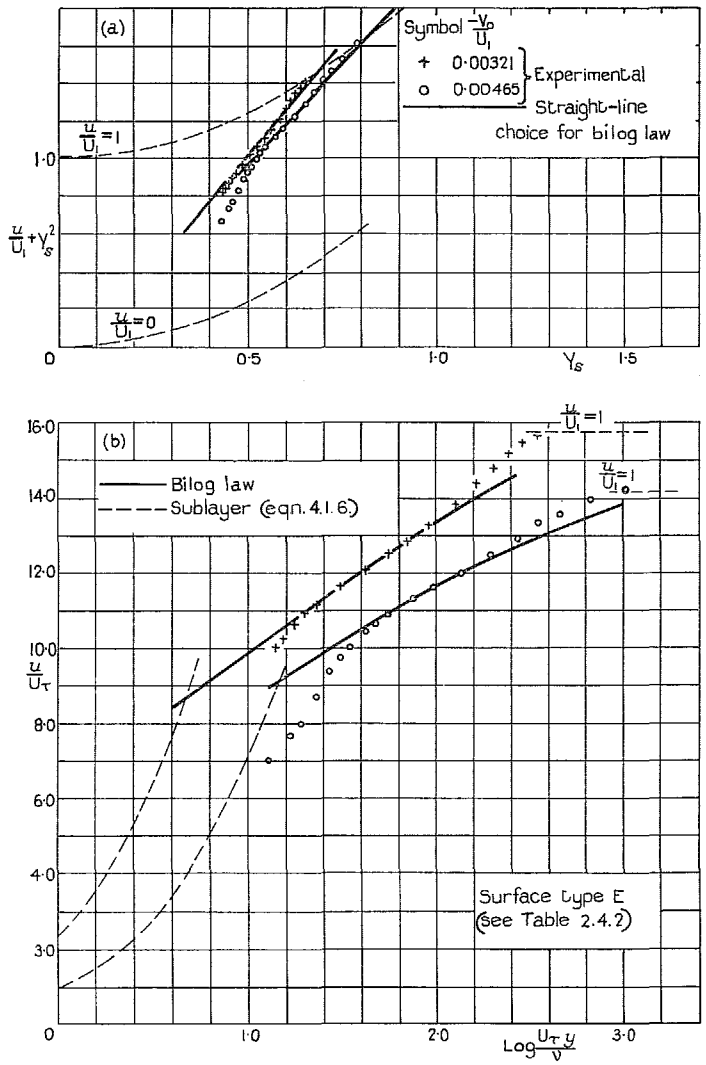

FIG. 8. Velocity profiles obtained by Black with suction through a blotting-paper surface.

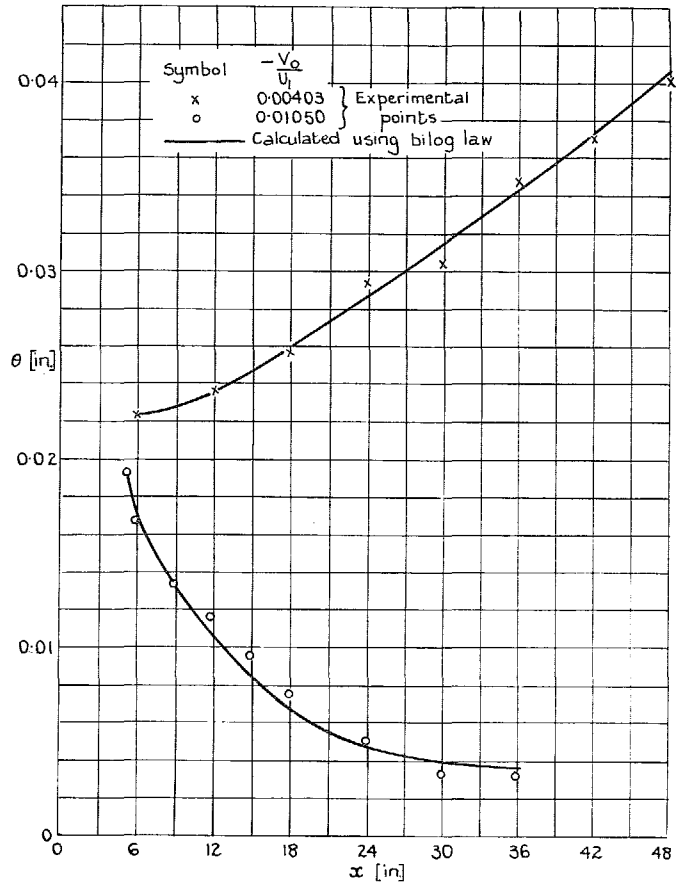

FIG. 9. Development of momentum thickness (Dutton's results with suction through a nylon surface).

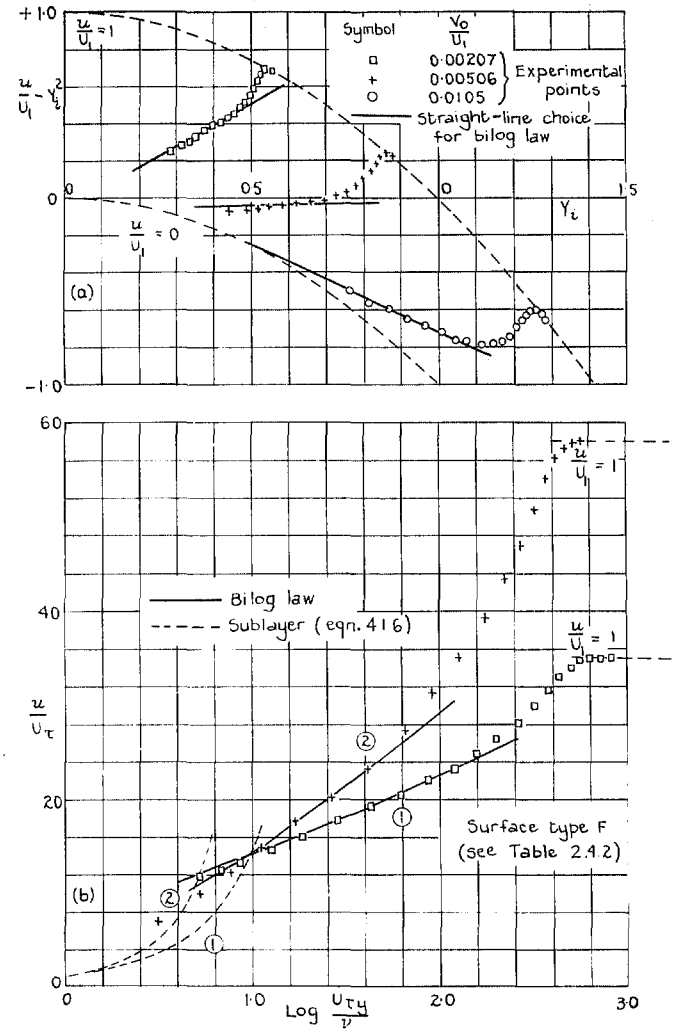

FIG. 10. Velocity profiles obtained by Mickley *et al* with injection through a mesh surface.

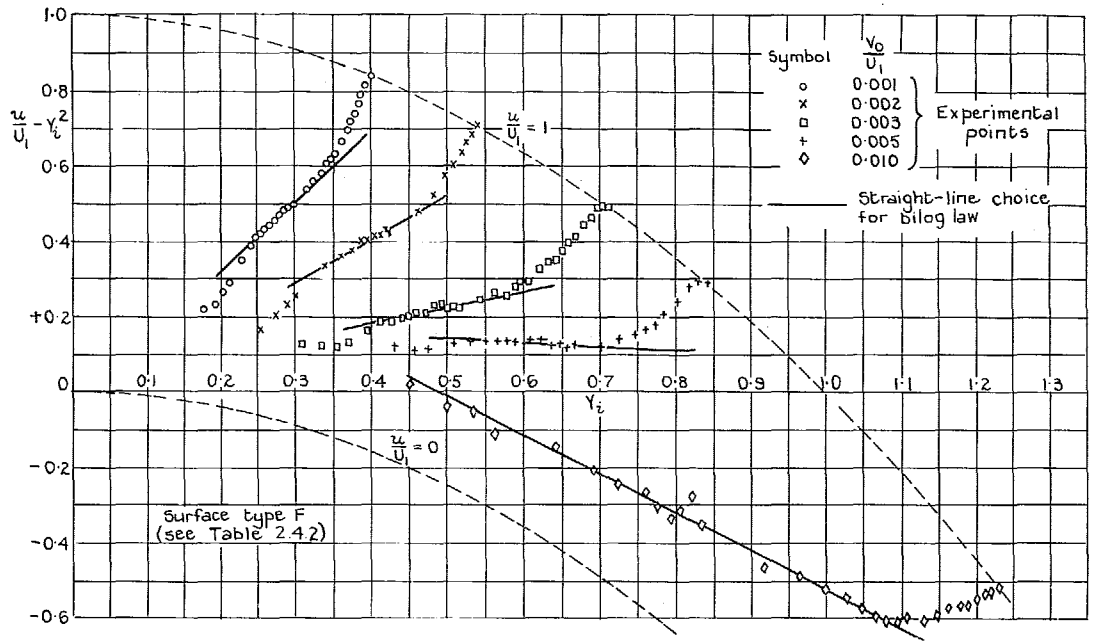

FIG. 11a. Velocity profiles obtained by Mickley with injection through a mesh surface.

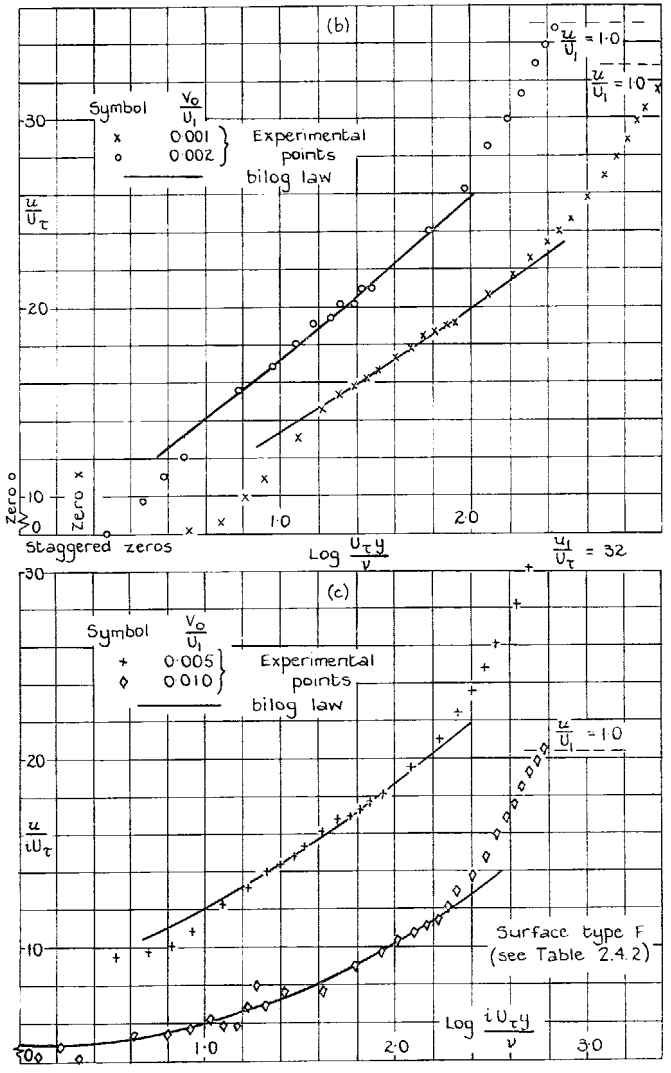

FIGS. 11b and c. Velocity profiles obtained by Mickley with injection through a mesh surface.

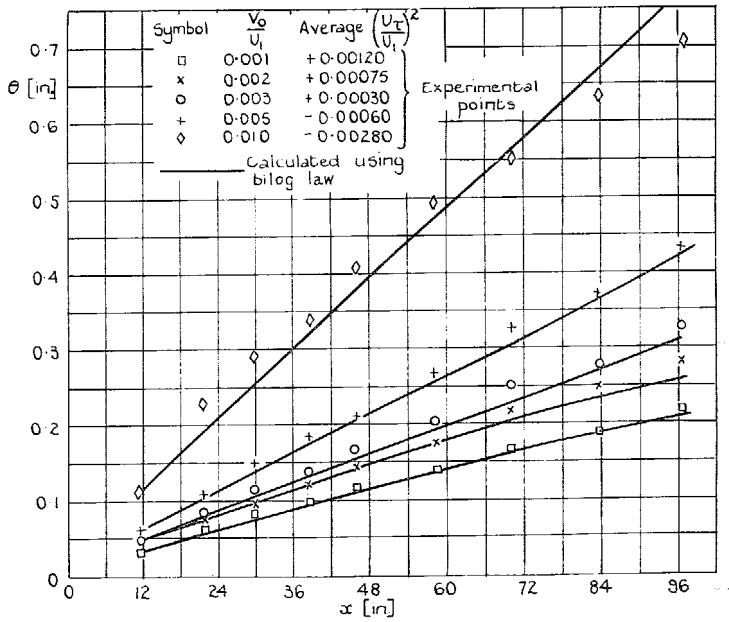

FIG. 12. Development of momentum thickness (Mickley's results with injection through a mesh surface).

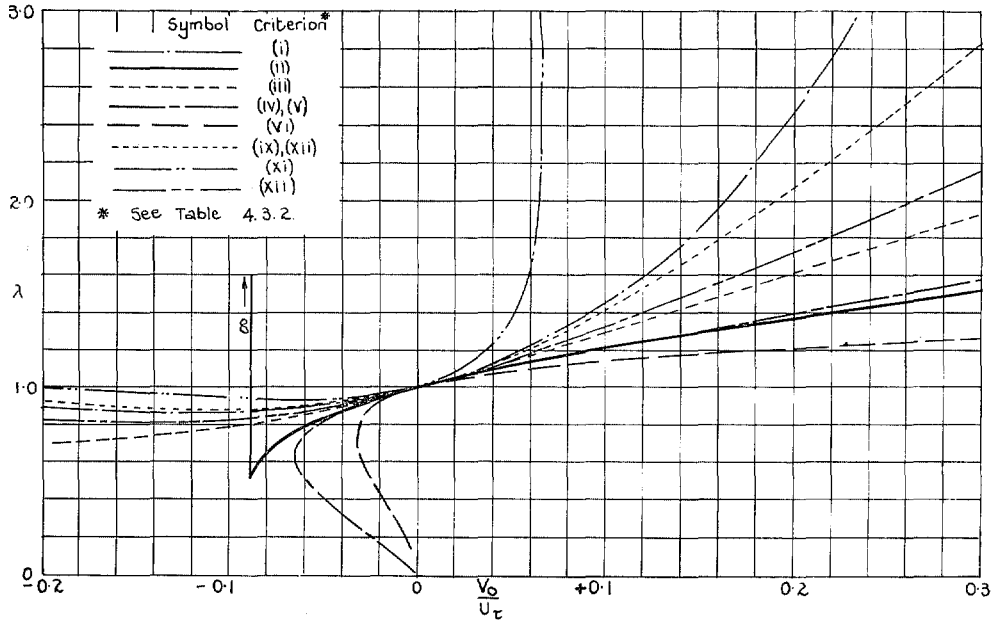

FIG. 13a. Variation of λ with v_0/U_τ as predicted by various transition criteria.

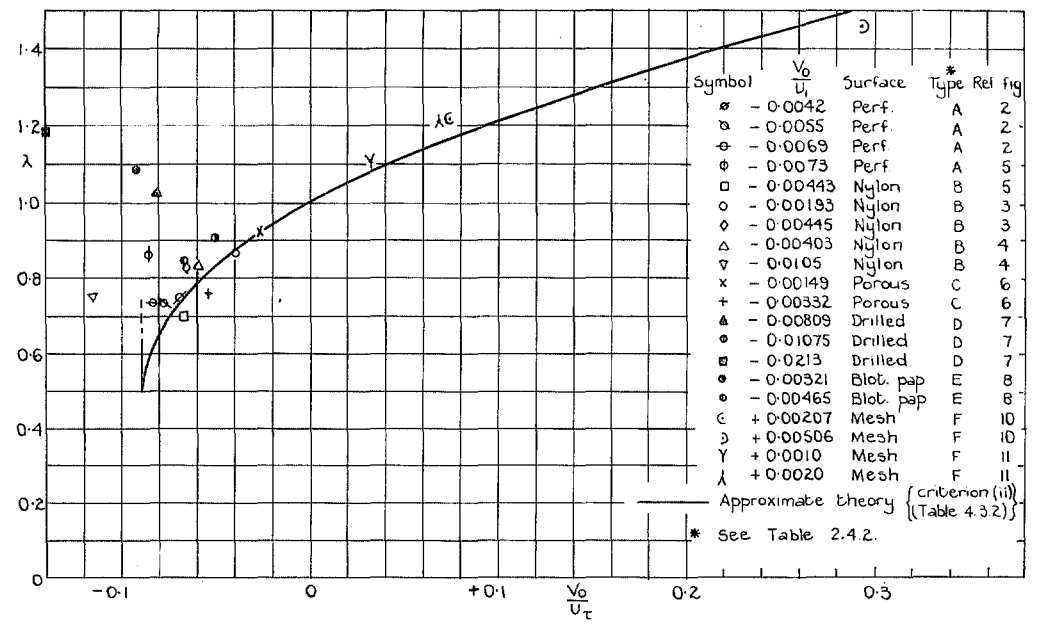

FIG. 13b. Variation of the profile parameter λ with v_0/U_τ.

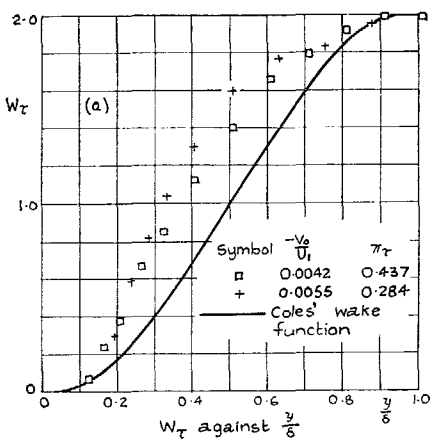

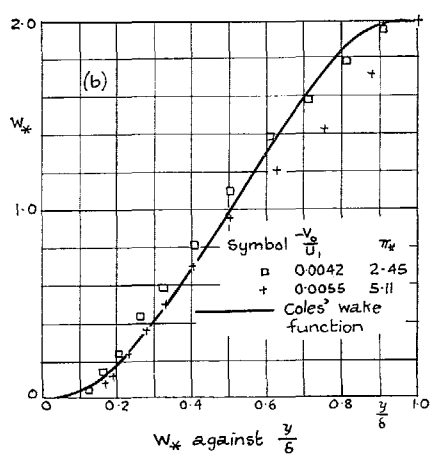

FIG. 14. Law of the wake with suction (Ref. Fig. 2). Surface type A (*see* Table 2.4.2).

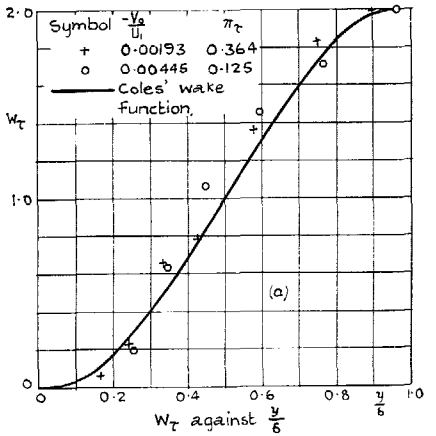

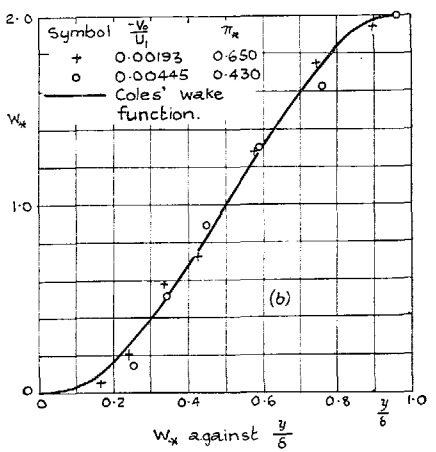

FIG. 15. Law of the wake with suction (Ref. Fig. 2). Surface type B (*see* Table 2.4.2).

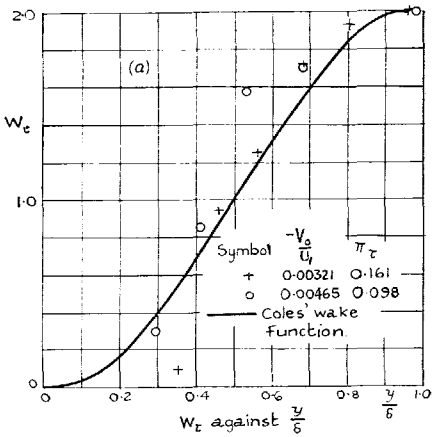

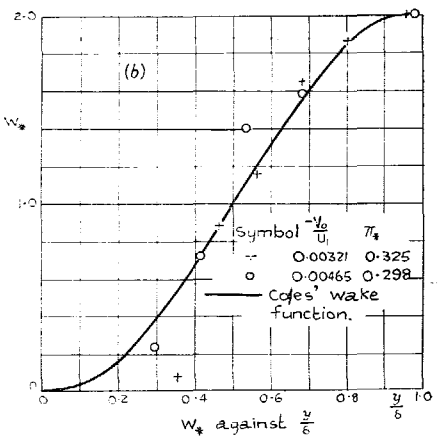

FIG. 16. Law of the wake with suction (Ref. Fig. 8). Surface type E (*see* Table 2.4.2).

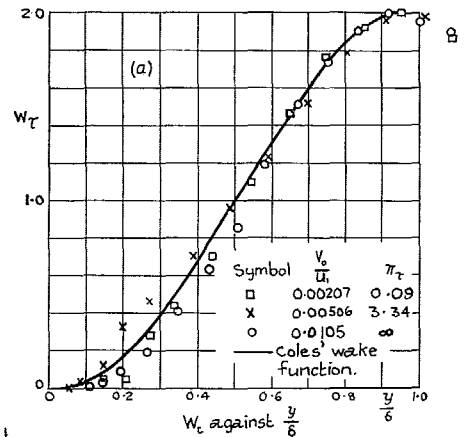

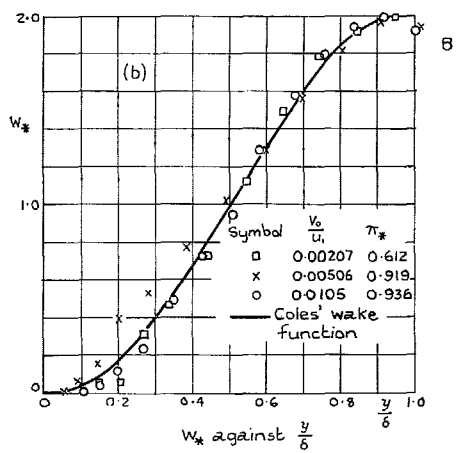

FIG. 17. Law of the wake with injection (Ref. Fig. 9). Surface type F (*see* Table 2.4.2).

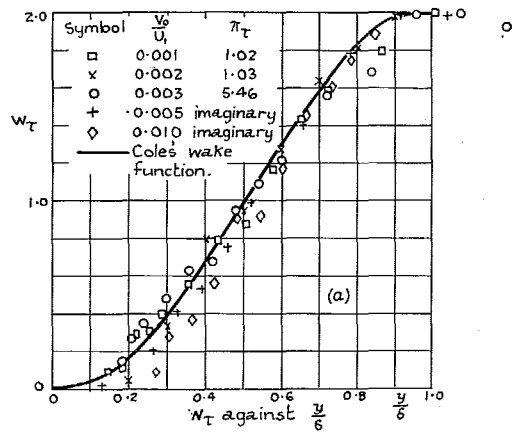

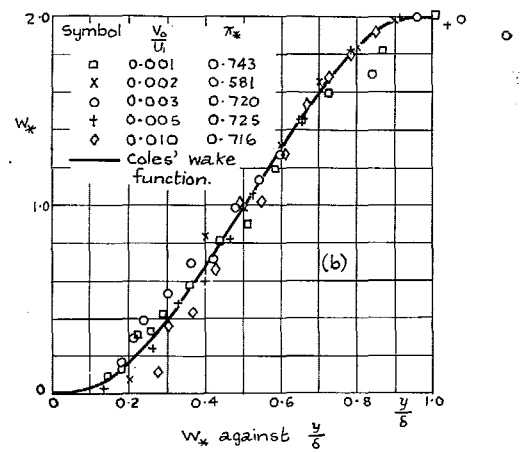

FIG. 18. Law of the wake with injection (Ref. Fig. 10). Surface type F (*see* Table 2.4.2).

(90747) Wt. 66/2301 K.5 3/65 Hw.

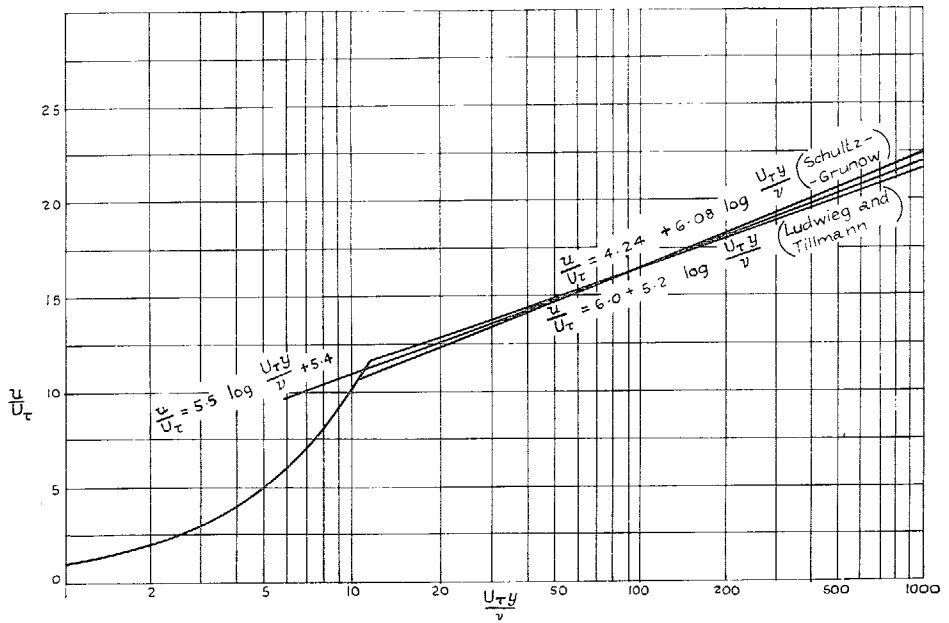

FIG. 19. Choice of constants in logarithmic law.

Publications of the Aeronautical Research Council

ANNUAL TECHNICAL REPORTS OF THE AERONAUTICAL RESEARCH COUNCIL (BOUND VOLUMES)

1945 Vol. I. Aero and Hydrodynamics, Aerofoils. £6 10s. (£6 13s. 6d.)
Vol. II. Aircraft, Airscrews, Controls. £6 10s. (£6 13s. 6d.)
Vol. III. Flutter and Vibration, Instruments, Miscellaneous, Parachutes, Plates and Panels, Propulsion. £6 10s. (£6 13s. 6d.)
Vol. IV. Stability, Structures, Wind Tunnels, Wind Tunnel Technique. £6 10s. (£6 13s. 3d.)

1946 Vol. I. Accidents, Aerodynamics, Aerofoils and Hydrofoils. £8 8s. (£8 11s. 9d.)
Vol. II. Airscrews, Cabin Cooling, Chemical Hazards, Controls, Flames, Flutter, Helicopters, Instruments and Instrumentation, Interference, Jets, Miscellaneous, Parachutes. £8 8s. (£8 11s. 3d.)
Vol. III. Performance, Propulsion, Seaplanes, Stability, Structures, Wind Tunnels. £8 8s. (£8 11s. 6d.)

1947 Vol. I. Aerodynamics, Aerofoils, Aircraft. £8 8s. (£8 11s. 9d.)
Vol. II. Airscrews and Rotors, Controls, Flutter, Materials, Miscellaneous, Parachutes, Propulsion, Seaplanes, Stability, Structures, Take-off and Landing. £8 8s. (£8 11s. 9d.)

1948 Vol. I. Aerodynamics, Aerofoils, Aircraft, Airscrews, Controls, Flutter and Vibration, Helicopters, Instruments, Propulsion, Seaplane, Stability, Structures, Wind Tunnels. £6 10s. (£6 13s. 3d.)
Vol. II. Aerodynamics, Aerofoils, Aircraft, Airscrews, Controls, Flutter and Vibration, Helicopters, Instruments, Propulsion, Seaplane, Stability, Structures, Wind Tunnels. £5 10s. (£5 13s. 3d.)

1949 Vol. I. Aerodynamics, Aerofoils. £5 10s. (£5 13s. 3d.)
Vol. II. Aircraft, Controls, Flutter and Vibration, Helicopters, Instruments, Materials, Seaplanes, Structures, Wind Tunnels. £5 10s. (£5 13s.)

1950 Vol. I. Aerodynamics, Aerofoils, Aircraft. £5 12s. 6d. (£5 16s.)
Vol. II. Apparatus, Flutter and Vibration, Meteorology, Panels, Performance, Rotorcraft, Seaplanes. £4 (£4 3s.)
Vol. III. Stability and Control, Structures, Thermodynamics, Visual Aids, Wind Tunnels. £4 (£4 2s. 9d.)

1951 Vol. I. Aerodynamics, Aerofoils. £6 10s. (£6 13s. 3d.)
Vol. II. Compressors and Turbines, Flutter, Instruments, Mathematics, Ropes, Rotorcraft, Stability and Control, Structures, Wind Tunnels. £5 10s. (£5 13s. 3d.)

1952 Vol. I. Aerodynamics, Aerofoils. £8 8s. (£8 11s. 3d.)
Vol. II. Aircraft, Bodies, Compressors, Controls, Equipment, Flutter and Oscillation, Rotorcraft, Seaplanes, Structures. £5 10s. (£5 13s.)

1953 Vol. I. Aerodynamics, Aerofoils and Wings, Aircraft, Compressors and Turbines, Controls. £6 (£6 3s. 3d.)
Vol. II. Flutter and Oscillation, Gusts, Helicopters, Performance, Seaplanes, Stability, Structures, Thermodynamics, Turbulence. £5 5s. (£5 8s. 3d.)

1954 Aero and Hydrodynamics, Aerofoils, Arrester gear, Compressors and Turbines, Flutter, Materials, Performance, Rotorcraft, Stability and Control, Structures. £7 7s. (£7 10s. 6d.)

Special Volumes

Vol. I. Aero and Hydrodynamics, Aerofoils, Controls, Flutter, Kites, Parachutes, Performance, Propulsion, Stability. £6 6s. (£6 9s.)
Vol. II. Aero and Hydrodynamics, Aerofoils, Airscrews, Controls, Flutter, Materials, Miscellaneous, Parachutes, Propulsion, Stability, Structures. £7 7s. (£7 10s.)
Vol. III. Aero and Hydrodynamics, Aerofoils, Airscrews, Controls, Flutter, Kites, Miscellaneous, Parachutes, Propulsion, Seaplanes, Stability, Structures, Test Equipment. £9 9s. (£9 12s. 9d.)

Reviews of the Aeronautical Research Council

1949–54 5s. (5s. 5d.)

Index to all Reports and Memoranda published in the Annual Technical Reports

1909–1947 R. & M. 2600 (out of print)

Indexes to the Reports and Memoranda of the Aeronautical Research Council

Between Nos. 2451–2549: R. & M. No. 2550 2s. 6d. (2s. 9d.); Between Nos. 2651–2749: R. & M. No. 2750 2s. 6d. (2s. 9d.); Between Nos. 2751–2849: R. & M. No. 2850 2s. 6d. (2s. 9d.); Between Nos. 2851–2949: R. & M. No. 2950 3s. (3s. 3d.); Between Nos. 2951–3049: R. & M. No. 3050 3s. 6d. (3s. 9d.); Between Nos. 3051–3149: R. & M. No. 3150 3s. 6d. (3s. 9d.); Between Nos. 3151–3249: R. & M. No. 3250 3s. 6d. (3s. 9d.); Between Nos. 3251–3349: R. & M. No. 3350 3s. 6d. (3s. 10d.)

Prices in brackets include postage

Government publications can be purchased over the counter or by post from the Government Bookshops in London, Edinburgh, Cardiff, Belfast, Manchester, Birmingham and Bristol, or through any bookseller

Printed and published by
HER MAJESTY'S STATIONERY OFFICE

To be purchased from
York House, Kingsway, London W.C.2
423 Oxford Street, London W.1
13A Castle Street, Edinburgh 2
109 St. Mary Street, Cardiff
39 King Street, Manchester 2
50 Fairfax Street, Bristol 1
35 Smallbrook, Ringway, Birmingham 5
80 Chichester Street, Belfast 1
or through any bookseller

Printed in England

S.O. Code No. 23-3387